

Models of radiative linear seesaw with electrically charged mediators

A. E. Cárcamo Hernández^{a,b,c,*}, Yocelyne Hidalgo Velásquez^{a,†},
Sergey Kovalenko^{c,d,‡}, Nicolás A. Pérez-Julve^{a,§} and Ivan Schmidt^{a,b,¶}

^a *Universidad Técnica Federico Santa María,
Casilla 110-V, Valparaíso, Chile*

^b *Centro Científico-Tecnológico de Valparaíso,
Casilla 110-V, Valparaíso, Chile*

^c *Millennium Institute for Subatomic Physics at the High-Energy Frontier, SAPHIR, Chile*

^d *Universidad Andrés Bello, Facultad de Ciencias Exactas,
Departamento de Ciencias Físicas-Center for Theoretical and Experimental Particle Physics,
Fernández Concha 700, Santiago, Chile*

(Dated: July 31, 2024)

We propose two versions of radiative linear seesaw models, where electrically charged scalars and vector-like leptons generate the Dirac neutrino mass submatrix at one and two loop levels. In these models, the SM charged lepton masses are generated from a one loop level radiative seesaw mechanism mediated by charged exotic vector-like leptons and electrically neutral scalars running in the loops. These models can successfully accommodate the current amount of dark matter and baryon asymmetries observed in the Universe, as well as the muon anomalous magnetic moment.

Our friend and collaborator Iván Schmidt passed away during the completion of this work. He will be sorely missed.

I. INTRODUCTION

The origin of the SM charged fermion mass hierarchy, the tiny active neutrino masses and the current amount of dark matter relic density and lepton asymmetries observed in the Universe are one of the most relevant open issues not addressed by the Standard Model (SM) of Particle Physics. Several theories have been proposed in order to explain the tiny values of the light active neutrino masses; see *e.g.* Ref. [1] for a review and [2] for a comprehensive study of one loop radiative neutrino mass models. The most economical way to generate the tiny masses of the light active neutrinos, considering the SM gauge symmetry, is by adding two right-handed Majorana neutrinos that mix with the light active neutrinos, thus triggering a canonical seesaw mechanism [3–9], where either the right handed Majorana neutrinos have to be extremely heavy, with masses of the order of the Grand Unification scale, or they can be around the TeV scale thus implying that the Dirac Yukawa couplings have to be very tiny. In both scenarios, the mixing between the active and sterile neutrinos is very tiny, leading to strongly suppressed charged lepton flavor (CLFV) violating signatures, several orders of magnitude below the experimental sensitivity, thus making this scenario untestable via CLFV decays. One interesting and testable explanation for the tiny masses of light active neutrinos is the so-called linear seesaw mechanism [10–25], in which the masses of light active neutrinos feature a linear dependence on the Dirac neutrino mass submatrix. In the linear seesaw realizations the mixing between active and sterile neutrinos is several orders of magnitudes larger than in the type I seesaw, thus resulting in charged lepton flavor violating decay

*Electronic address: antonio.carcamo@usm.cl

†Electronic address: yocehidalgo@gmail.com

‡Electronic address: sergey.kovalenko@unab.cl

§Electronic address: nicolasperezjulve@gmail.com

¶Electronic address: [Deceased](#)

rates within the reach of experimental sensitivity. Furthermore, the linear seesaw realizations, due to the small mass splitting between the heavy pseudoDirac neutral leptons, provides a successful scenario for resonant leptogenesis.

In the present paper we propose a radiative realization of the linear seesaw mechanism, where the Dirac neutrino mass submatrix is generated at one or two loop level. The layout of the remainder of the paper is as follows. In section II we describe two radiative linear seesaw models, where the Dirac neutrino mass matrix is generated at one and two loops. The implications of the two loop radiative linear seesaw model in leptogenesis is discussed in section VIII. The consequences of the radiative linear seesaw models in muon anomalous magnetic moment, dark matter, charged lepton flavor violation and leptogenesis are discussed in sections V, VI, VII and VIII, respectively. We state our conclusions in section IX. Appendix A shows in full detail the perturbative diagonalization procedure of the full 7×7 neutrino mass matrix.

II. THE MODELS

In this section we discuss two radiative linear seesaw models where the Dirac neutrino mass matrix is generated at one and two loops from the virtual exchange of electrically charged mediators. We discuss the phenomenological consequences of these models for the muon anomalous magnetic moment. Before describing two radiative linear seesaw models, where the Dirac neutrino mass matrix is generated at one and two loops, we start by explaining the motivations behind the inclusion of extra scalars, fermions and symmetries needed for implementing the linear seesaw mechanism at one and two loop levels and to generate the SM charged lepton masses at one loop level. The masses of the active light neutrinos arise from a linear seesaw mechanism when the full neutrino mass matrix expressed in the basis (ν_L, ν_R^C, N_R^C) , has the following structure:

$$M_\nu = \begin{pmatrix} 0_{3 \times 3} & \varepsilon & m \\ \varepsilon^T & 0_{2 \times 2} & M \\ m^T & M^T & 0_{2 \times 2} \end{pmatrix}, \quad (1)$$

where ν_{iL} ($i = 1, 2, 3$) are active neutrinos, whereas ν_{kR} and N_{kR} ($k = 1, 2$) are the sterile neutrinos. Their lepton numbers are $L(\nu_L) = L(\nu_R) = -L(N_R) = 1$. Therefore, the only source of lepton number violation is m -entry. For the linear seesaw mechanism to work properly, the entries of the full neutrino mass matrix (1) should obey the hierarchy $\varepsilon_{in} \ll m_{in} \ll M_{np}$ ($i = 1, 2, 3, n, p = 1, 2$). In what follows we will discuss the models where the smallness of the submatrix ε is due to symmetries allowing its generation only at one- and two-loop levels.

We first explain how the tree level type I and tree level linear seesaw mechanisms are forbidden in our models. This is done by precluding certain operators with ad hoc symmetries imposed on the models. To forbid the tree level type I seesaw mechanism, we look for a symmetry forbidding the operators:

$$\bar{l}_{iL} \tilde{\phi} \nu_{nR}, \quad m_{\nu_R} \bar{\nu}_{mR} \nu_{nR}^C \quad (2)$$

whereas in the case of linear seesaw mechanism it is sufficient to ban only one of the following operators:

$$\bar{l}_{iL} \tilde{\phi} \nu_{nR}, \quad \bar{l}_{iL} \tilde{\phi} N_{nR}, \quad m_{\nu_R} \bar{\nu}_{mR} N_{nR}^C. \quad (3)$$

Here ϕ is the SM Higgs doublet, l_{iL} ($i = 1, 2, 3$) stand for the SM leptonic doublets, while ν_{nR} and N_{nR} ($n = 1, 2, 3$) are gauge singlets right handed Majorana neutrinos. We choose to ban the $\bar{l}_{iL} \tilde{\phi} \nu_{nR}$ Yukawa operator, whereas allowing the $\bar{l}_{iL} \tilde{\phi} N_{nR}$ and $m_{\nu_R} \bar{\nu}_{mR} N_{nR}^C$ operators. To implement the above specified conditions we impose on the model a Z_4 discrete symmetry, which is assumed to be spontaneously broken down to a preserved \tilde{Z}_2 discrete symmetry. This guarantees the radiative nature of the linear seesaw mechanism, where the submatrix ε arises at one loop level. In this approach we also need to extend the SM scalar sector by adding an inert $SU(2)_L$ scalar doublet η , two pairs

of electrically charged scalar singlets S_1^\pm, S_2^\pm , two electrically neutral scalar singlets χ, ξ and three $SU(2)_L$ singlet charged vector-like leptons E_i ($i = 1, 2, 3$). With these fields we can build the following operators needed for the construction of the submatrix ε at one loop level:

$$\bar{l}_{iL}\eta E_{jR}, \quad \bar{E}_{iL}S_1^-\nu_{nR}, \quad (M_E)_{ij}\bar{E}_{iL}E_{jR}, \quad S_1^+S_2^-\chi\xi, \quad \varepsilon_{ab}(\eta^*)^a(\phi^*)^b S_2^+. \quad (4)$$

For generating the submatrices m and M , one has to introduce the operators:

$$\bar{l}_{iL}\tilde{\phi}N_{nR}, \quad M_{mn}\bar{\nu}_{mR}N_{nR}^C \quad (5)$$

Let us note, that several of the above-introduced fields

play an important role in the one loop level radiative seesaw mechanism that generates the SM charged fermion masses.

For this, it is additionally necessary to introduce an electrically neutral scalar singlet ρ and three charged exotic leptons E_i ($i = 1, 2, 3$), as well as right-handed Majorana neutrinos N_{nR} and ν_{nR} ($n = 1, 2$) in the singlet $SU(2)$ representations. The charged exotic leptons E_i ($i = 1, 2, 3$) mediate a one loop level radiative seesaw mechanism that gives rise to the SM charged lepton masses and to the neutrino mass submatrix ε . This mechanism can be implemented via the following operators:

$$\bar{l}_{iL}\eta E_{jR}, \quad \bar{E}_{iL}\rho l_{jR}, \quad \eta^\dagger\phi\rho, \quad (\rho^*)^2\chi\xi, \quad (M_E)_{ij}\bar{E}_{iL}E_{jR}, \quad (6)$$

To guarantee the radiative nature of the above described seesaw mechanisms, we need to add the spontaneously broken Z_2 and Z_4 discrete symmetries, with Z_4 broken down to a residual \tilde{Z}_2 discrete symmetry preserved at low energies. Furthermore, the inclusion of the Z_4 symmetry will be crucial to forbid the Majorana mass terms $M_{mn}^{(\nu)}\bar{\nu}_{mR}\nu_{nR}^C$ and $M_{mn}^{(N)}\bar{N}_{mR}N_{nR}^C$, thus allowing us to have zero 2×2 submatrices in Eq. (1). We assume that the inert $SU(2)$ doublet η and the singlet scalar ρ have complex Z_4 charges, thus implying that they will be charged under the residual \tilde{Z}_2 symmetry. The inclusions of these inert fields is necessary to radiatively generate the SM charged lepton mass matrix at one loop level. To close the corresponding loop, the scalar singlets χ and ξ , having real Z_4 charges, are required in the scalar spectrum. Besides that, the radiative seesaw mechanism that generates the submatrix ε at one loop level is mediated by the above mentioned inert doublet η , as well as by the electrically charged scalar singlets S_1^\pm and S_2^\pm , whose inclusion is necessary for the implementation of this mechanism.

Now we proceed to discuss the case where the submatrix ε is generated at two loop level.

This requires introduction of six charged exotic leptons E_i, \tilde{E}_i ($i = 1, 2, 3$), right handed Majorana neutrinos N_{nR} and ν_{nR} ($n = 1, 2$) in the singlet representations of $SU(2)$ as well as inert $SU(2)$ doublet scalar η , and gauge singlet scalars $\chi, \xi, \sigma, S_1^\pm, S_2^\pm$. Generation of the submatrix ε at two loop level requires the inclusion of the following operators:

$$\bar{l}_{iL}\eta E_{jR}, \quad \bar{E}_{iL}S_1^-\nu_{nR}, \quad (M_E)_{ij}\bar{E}_{iL}E_{jR}, \quad \bar{E}_{iL}\sigma\tilde{E}_{jR}, \quad (M_{\tilde{E}})_{ij}\bar{\tilde{E}}_{iL}\tilde{E}_{jR}, \quad S_1^+S_2^-\chi\xi, \quad \varepsilon_{ab}(\eta^*)^a(\phi^*)^b S_2^+\sigma^* \quad (7)$$

The condition that the submatrix ε appears only at the two-loop level requires introduction of the conserved discrete $Z_2^{(2)}$ symmetry as well as of the spontaneously broken $Z_2^{(1)}$ and Z_4 discrete symmetries, with Z_4 assumed to be broken down to a preserved \tilde{Z}_2 discrete symmetry. In comparison with the previously discussed one-loop realization, here we need an extra preserved discrete $Z_2^{(2)}$ symmetry in order to prevent one-loop radiative generation of the submatrix ε . Note that in this realization of the two-loop linear seesaw mechanism, the masses of charged SM fermions are generated in exactly the same way as in the previously described one-loop case.

A. Model 1: One-loop radiative linear seesaw model

We consider an extended Inert Doublet Model (IDM), where the scalar content is enlarged by the inclusion of several gauge singlet scalars, whereas the lepton sector is augmented by considering right handed Majorana neutrinos and

charged exotic vector like leptons. The SM gauge symmetry is extended by the inclusion of the spontaneously broken $Z_2 \times Z_4$ discrete symmetry. The Z_4 discrete symmetry is broken down to a preserved \tilde{Z}_2 discrete symmetry, which is a stabilizer of Dark Matter (DM) particle candidate. Schematically, the symmetry breaking chain goes as follows,

$$\begin{aligned}
\mathbb{G}_1 &= SU(3)_C \times SU(2)_L \times U(1)_Y \times Z_2 \times Z_4 \\
&\quad \Downarrow v_\xi, v_\chi \\
&= SU(3)_C \times SU(2)_L \times U(1)_Y \times \tilde{Z}_2 \\
&\quad \Downarrow v \\
&= SU(3)_C \times U(1)_{\text{em}} \times \tilde{Z}_2
\end{aligned} \tag{8}$$

where $\tilde{Z}_2 \subset Z_4$. The SM Higgs VEV we denoted as $\langle \phi^0 \rangle = v/\sqrt{2}$. The global $Z_2 \times Z_4$ discrete symmetry is spontaneously broken at the TeV scale by the vacuum expectation values (VEVs) of the gauge singlet scalars $\langle \xi \rangle = v_\xi$, $\langle \chi \rangle = v_\chi$.

The scalar and leptonic fields with their assignments under the model symmetry group \mathbb{G}_1 are shown in Tables I and II, respectively. This defines the leptonic Yukawa interaction in this model

$$\begin{aligned}
-\mathcal{L}_Y^{(l)} &= \sum_{i=1}^3 \sum_{j=1}^3 y_{ij}^{(E)} \bar{l}_{iL} \eta E_{jR} + \sum_{i=1}^3 \sum_{j=1}^3 x_{ij}^{(l)} \bar{E}_{iL} \rho l_{jR} + \sum_{i=1}^3 \sum_{n=1}^2 x_{in}^{(\nu)} \bar{E}_{iL} S_1^- \nu_{nR} + \sum_{i=1}^3 \sum_{n=1}^2 y_{in}^{(N)} \bar{l}_{iL} \tilde{\phi} N_{nR} \\
&\quad + \sum_{m=1}^2 \sum_{n=1}^2 M_{mn} \bar{\nu}_{mR} N_{nR}^C + \sum_{i=1}^3 \sum_{j=1}^3 (M_E)_{ij} \bar{E}_{iL} E_{jR} + h.c
\end{aligned} \tag{9}$$

Note that the residual \tilde{Z}_2 discrete symmetry is preserved at low energies since we require that the $SU(2)_L$ doublet scalar η and the scalar singlets ρ do not develop vacuum expectation values. As we will show in subsequent sections a viable DM candidate is the lightest among the \tilde{Z}_2 -odd scalar fields $\text{Re } \eta^0$, $\text{Im } \eta^0$, $\text{Re } \rho$, $\text{Im } \rho$.

Furthermore, the electrically charged components of the $SU(2)_L$ doublet scalar η , together with the electrically charged gauge singlet scalars S_1^- , S_2^- and the vector like leptons E_i ($i = 1, 2, 3$) will induce a one loop level radiative seesaw mechanism that generates the Dirac neutrino mass matrix, as shown in the Feynman diagram of Figure 2. We further include right handed Majorana neutrinos ν_{nR} , N_{nR} ($n = 1, 2$) (having opposite Z_4 charges), in order to implement a one loop level radiative linear seesaw mechanism that produces the tiny masses of the light active neutrinos. Furthermore, the heavy vector like leptons E_i ($i = 1, 2, 3$), induce a radiative seesaw mechanism at one loop level that generates the SM charged lepton masses. It is worth mentioning that having three vector like leptons E_i ($i = 1, 2, 3$), singlets under $SU(2)_L$, is the minimal amount of charged exotic leptons needed to generate the SM charged lepton masses. Furthermore, the extra $Z_2 \times Z_4$ discrete symmetry selects the allowed entries of the full neutrino mass matrix, thus allowing a successful implementation of the linear seesaw mechanism that produces the light active neutrino masses.

B. Model 2: Two-loop radiative linear seesaw model

Now we consider an extension of the previously described one loop radiative linear seesaw model, where the masses of the light active neutrinos appear at two loop level. The scalar and leptonic content will be similar to the previous model. In addition to the fields considered there, we introduce charged exotic vector like leptons \tilde{E}_i ($i = 1, 2, 3$) as well as the electrically neutral gauge singlet scalar σ , assumed to be charged under a preserved $Z_2^{(2)}$ symmetry.

The SM gauge symmetry is supplemented by the inclusion of the $Z_2^{(1)} \times Z_2^{(2)} \times Z_4$ discrete group. The full symmetry

| | $SU(3)_C$ | $SU(2)_L$ | $U(1)_Y$ | Z_2 | Z_4 | \tilde{Z}_2 |
|-----------|-----------|-----------|---------------|-------|---------|---------------|
| ϕ | 1 | 2 | $\frac{1}{2}$ | 1 | 1 | 1 |
| η | 1 | 2 | $\frac{1}{2}$ | 1 | i | -1 |
| ρ | 1 | 1 | 0 | 1 | i | -1 |
| ξ | 1 | 1 | 0 | -1 | -1 | 1 |
| χ | 1 | 1 | 0 | -1 | 1 | 1 |
| S_1^\pm | 1 | 1 | ± 1 | 1 | $\mp i$ | -1 |
| S_2^\pm | 1 | 1 | ± 1 | 1 | $\pm i$ | -1 |

Table I: Model 1. Scalar assignments under $\mathbb{G}_1 = SU(3)_C \times SU(2)_L \times U(1)_Y \times Z_2 \times Z_4$ symmetry in the one loop radiative linear seesaw model.

| | $SU(3)_C$ | $SU(2)_L$ | $U(1)_Y$ | Z_2 | Z_4 | \tilde{Z}_2 |
|------------|-----------|-----------|----------------|-------|-------|---------------|
| l_{iL} | 1 | 2 | $-\frac{1}{2}$ | 1 | $-i$ | -1 |
| l_{iR} | 1 | 1 | -1 | 1 | i | -1 |
| ν_{nR} | 1 | 1 | 0 | 1 | i | -1 |
| N_{nR} | 1 | 1 | 0 | 1 | $-i$ | -1 |
| E_{iL} | 1 | 1 | -1 | 1 | -1 | 1 |
| E_{iR} | 1 | 1 | -1 | 1 | -1 | 1 |

Table II: Model 1. Lepton assignments under $\mathbb{G}_1 = SU(3)_C \times SU(2)_L \times U(1)_Y \times Z_2 \times Z_4$ symmetry in the one loop radiative linear seesaw model.

\mathbb{G} of the model exhibits the following breaking scheme

$$\begin{aligned}
\mathbb{G}_2 &= SU(3)_C \times SU(2)_L \times U(1)_Y \times Z_2^{(1)} \times Z_2^{(2)} \times Z_4 & (10) \\
&\quad \Downarrow v_\xi, v_\chi \\
&SU(3)_C \times SU(2)_L \times U(1)_Y \times Z_2^{(2)} \times \tilde{Z}_2 \\
&\quad \Downarrow v \\
&SU(3)_C \times U(1)_{\text{em}} \times Z_2^{(2)} \times \tilde{Z}_2 & (11)
\end{aligned}$$

where $\tilde{Z}_2 \subset Z_4$. The scalar and leptonic fields and their assignments under the model symmetry group \mathbb{G} are shown in Tables III and IV, respectively. With this field content and symmetries we have the following relevant leptonic Yukawa interactions

$$\begin{aligned}
-\mathcal{L}_Y^{(l)} &= \sum_{i=1}^3 \sum_{j=1}^3 y_{ij}^{(E)} \bar{l}_{iL} \eta E_{jR} + \sum_{i=1}^3 \sum_{j=1}^3 x_{ij}^{(l)} \bar{E}_{iL} \rho l_{jR} + \sum_{i=1}^3 \sum_{n=1}^2 x_{in}^{(\nu)} \bar{E}_{iL} S_1^- \nu_{nR} + \sum_{i=1}^3 \sum_{n=1}^2 y_{in}^{(N)} \bar{l}_{iL} \tilde{\phi} N_{nR} & (12) \\
&+ \sum_{i=1}^3 \sum_{j=1}^3 x_{ij}^{(E)} \bar{E}_{iL} \sigma \tilde{E}_{jR} + \sum_{m=1}^2 \sum_{n=1}^2 M_{mn} \bar{\nu}_{mR} N_{nR}^C + \sum_{i=1}^3 \sum_{j=1}^3 (M_E)_{ij} \bar{E}_{iL} E_{jR} + \sum_{i=1}^3 \sum_{j=1}^3 (M_{\tilde{E}})_{ij} \bar{\tilde{E}}_{iL} \tilde{E}_{jR} + h.c.
\end{aligned}$$

In this model $Z_2^{(2)} \times \tilde{Z}_2$ discrete symmetry is preserved at low energies since we require that the $SU(2)_L$ doublet scalar η as well as the electrically neutral scalar singlets ρ and σ do not acquire vacuum expectation values.

As we will show in subsequent sections a viable DM candidate is the lightest among the \tilde{Z}_2 -odd scalar fields $\text{Re } \eta^0$, $\text{Im } \eta^0$, $\text{Re } \rho$, $\text{Im } \rho$, $\text{Re } \sigma$, $\text{Im } \sigma$.

| | $SU(3)_C$ | $SU(2)_L$ | $U(1)_Y$ | $Z_2^{(1)}$ | $Z_2^{(2)}$ | Z_4 | \tilde{Z}_2 |
|------------------|-----------|-----------|----------------|-------------|-------------|-------|---------------|
| l_{iL} | 1 | 2 | $-\frac{1}{2}$ | 1 | 1 | $-i$ | -1 |
| l_{iR} | 1 | 1 | -1 | 1 | 1 | i | -1 |
| ν_{nR} | 1 | 1 | 0 | 1 | 1 | i | -1 |
| N_{nR} | 1 | 1 | 0 | 1 | 1 | $-i$ | -1 |
| E_{iL} | 1 | 1 | -1 | 1 | 1 | -1 | 1 |
| E_{iR} | 1 | 1 | -1 | 1 | 1 | -1 | 1 |
| \tilde{E}_{iL} | 1 | 1 | -1 | 1 | -1 | -1 | 1 |
| \tilde{E}_{iR} | 1 | 1 | -1 | 1 | -1 | -1 | 1 |

Table III: Model 2. Lepton assignments under $\mathbb{G}_2 = SU(3)_C \times SU(2)_L \times U(1)_Y \times Z_2^{(1)} \times Z_2^{(2)} \times Z_4$ symmetry in the two loop radiative linear seesaw model.

| | $SU(3)_C$ | $SU(2)_L$ | $U(1)_Y$ | $Z_2^{(1)}$ | $Z_2^{(2)}$ | Z_4 | \tilde{Z}_2 |
|-----------|-----------|-----------|---------------|-------------|-------------|---------|---------------|
| ϕ | 1 | 2 | $\frac{1}{2}$ | 1 | 1 | 1 | 1 |
| η | 1 | 2 | $\frac{1}{2}$ | 1 | 1 | i | -1 |
| σ | 1 | 1 | 0 | 1 | -1 | 1 | 1 |
| ρ | 1 | 1 | 0 | 1 | 1 | i | -1 |
| ξ | 1 | 1 | 0 | -1 | 1 | -1 | 1 |
| χ | 1 | 1 | 0 | -1 | 1 | 1 | 1 |
| S_1^\pm | 1 | 1 | ± 1 | 1 | -1 | $\mp i$ | -1 |
| S_2^\pm | 1 | 1 | ± 1 | 1 | -1 | $\pm i$ | -1 |

Table IV: Model 2. Scalar assignments under $\mathbb{G}_2 = SU(3)_C \times SU(2)_L \times U(1)_Y \times Z_2^{(1)} \times Z_2^{(2)} \times Z_4$ symmetry in the two loop radiative linear seesaw model.

III. SCALAR POTENTIAL

In this section we analyze the scalar potential of model 1. The scalar potential invariant under the symmetries of the model has the form:

$$\begin{aligned}
V = & -\mu_\phi^2(\phi^\dagger\phi) - \mu_\eta^2(\eta^\dagger\eta) - \mu_\rho^2(\rho^\dagger\rho) - \mu_\xi^2(\xi^\dagger\xi) - \mu_\chi^2(\chi^\dagger\chi) + \lambda_1(\phi^\dagger\phi)(\phi^\dagger\phi) + \lambda_2(\eta^\dagger\eta)(\eta^\dagger\eta) \\
& + \lambda_3(\rho^\dagger\rho)(\rho^\dagger\rho) + \lambda_4(\xi^\dagger\xi)(\xi^\dagger\xi) + \lambda_5(\chi^\dagger\chi)(\chi^\dagger\chi) + \lambda_6(\phi^\dagger\eta)(\eta^\dagger\phi) + \lambda_7(\eta^\dagger\rho)(\rho^\dagger\eta) + \lambda_8(\eta^\dagger\eta)(\rho^\dagger\rho) \\
& + \lambda_9(\phi^\dagger\xi)(\xi^\dagger\phi) + \lambda_{10}(\phi^\dagger\chi)(\chi^\dagger\phi) + \lambda_{11}(\phi^\dagger\phi)(\xi^\dagger\xi) + \lambda_{12}(\phi^\dagger\phi)(\chi^\dagger\chi) + \lambda_{13}(\xi^\dagger\xi)(\chi^\dagger\chi) \\
& + \lambda_{14}(\xi^\dagger\chi)(\chi^\dagger\xi) + \lambda_{15}(\phi^\dagger\phi)(\eta^\dagger\eta) + \lambda_{16}(\phi^\dagger\phi)(\rho^\dagger\rho) + f(\eta^\dagger\phi\rho + \text{h.c}) + \lambda_{17}(\eta^\dagger\chi)(\chi^\dagger\eta) \\
& + \lambda_{18}(\rho^\dagger\chi)(\chi^\dagger\rho) + \lambda_{19}(\eta^\dagger\xi)(\xi^\dagger\eta) + \lambda_{20}(\rho^\dagger\xi)(\xi^\dagger\rho) + \lambda_{21}(\rho^2\xi\chi + \text{h.c})
\end{aligned} \tag{13}$$

where the $SU(2)_L$ scalar doublets are given by

$$\phi = \begin{pmatrix} \phi^\pm \\ \phi^0 \end{pmatrix}, \quad \eta = \begin{pmatrix} \eta^\pm \\ \eta^0 \end{pmatrix} \tag{14}$$

Here, ϕ is the SM Higgs doublet and η is the inert $SU(2)$ scalar doublet. The coupling terms of $\phi S_2 \eta$, $\eta \phi \sigma S_2$ and $S_2 S_1 \chi \xi$ are considered in the vertices of diagrams in Figure 2 and Figure 3 whereas in the scalar potential in Eq. (13) we consider the common terms in Model 1 and Model 2 to study phenomenological aspects like muon g-2 in Section V and dark matter in Section VI.

For finding constraints on the parameters λ_i from the condition that the scalar potential V is bounded from below, we just need to examine the quartic terms of the scalar potential as in [26]. Here we considered quartic terms in the

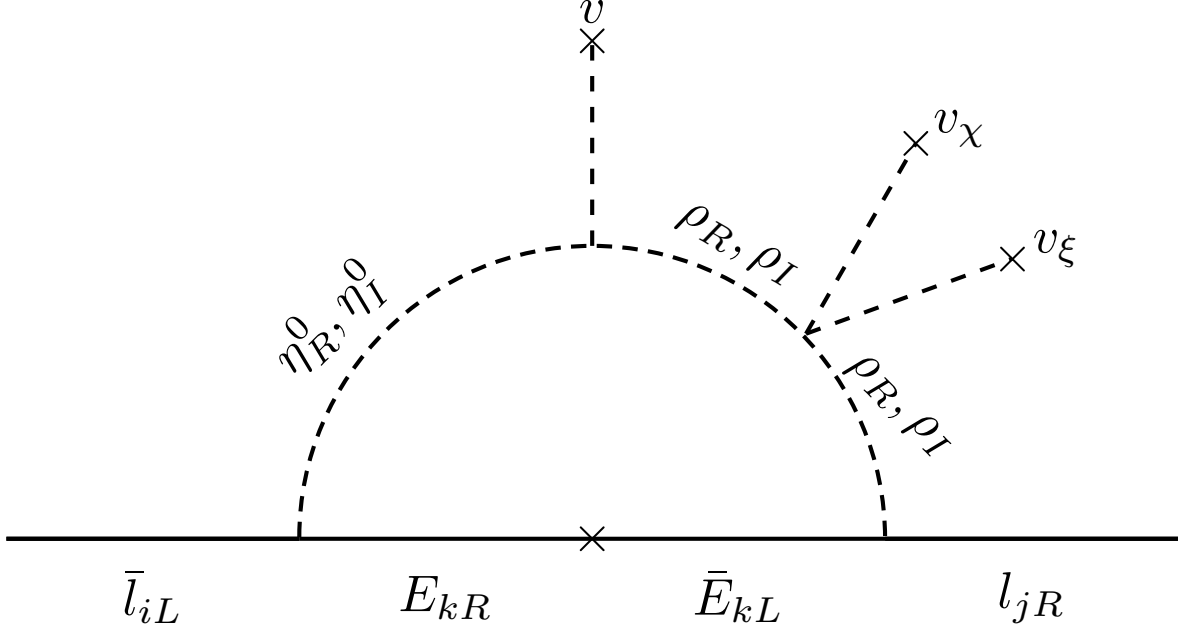


Figure 1: Models 1 and 2. One-loop Feynman diagram contributing to the charged lepton mass matrix. Here $i, j, k = 1, 2, 3$.

scalar potential that are relevant for $g - 2$ and Dark Matter phenomenology. For convenience we define $a = \phi^\dagger \phi$, $b = \eta^\dagger \eta$, $c = \rho^\dagger \rho$, $d = \Re(\phi^\dagger \eta)$, $e = \Im(\phi^\dagger \eta)$, $g = \Re(\eta^\dagger \rho)$, $h = \Im(\eta^\dagger \rho)$, $z = \eta^\dagger \phi \rho$, $j = \Re(\eta^\dagger \chi)$, $k = \Im(\eta^\dagger \chi)$, $l = \Re(\rho^\dagger \chi)$, $m = \Im(\rho^\dagger \chi)$, $n = \Re(\eta^\dagger \xi)$, $p = \Im(\eta^\dagger \xi)$, $q = \Re(\rho^\dagger \xi)$, $r = \Im(\rho^\dagger \xi)$, $x = \rho^2 \xi \chi$. With this notation we can write the quartic terms $V_4 \subset V$ as

$$\begin{aligned}
V_4 = & \left(\lambda_1^{1/2} a - \lambda_2^{1/2} b \right)^2 + \left(\lambda_2^{1/2} b - \lambda_3^{1/2} c \right)^2 + \left(\lambda_{15} + 2\lambda_1^{1/2} \lambda_2^{1/2} \right) (ab - d^2 - e^2) \\
& + (\lambda_8 + 2(\lambda_2 \lambda_3)^{1/2}) (bc - g^2 - h^2) + \left(\lambda_8 + \lambda_7 + 2(\lambda_2 \lambda_3)^{1/2} \right) (g^2 + h^2) \\
& + \left(\lambda_{15} + \lambda_6 + 2(\lambda_1 \lambda_2)^{1/2} \right) (d^2 + e^2) + \lambda_{16} (ac) + fz + \lambda_{17} (j^2 + k^2) \\
& + \lambda_{18} (l^2 + m^2) + \lambda_{19} (n^2 + p^2) + \lambda_{20} (q^2 + r^2) + \lambda_{21} (x + \text{h.c.})
\end{aligned}$$

We require that there are no directions in the field space along which $V \rightarrow -\infty$. This leads to the following constraints on the λ_i :

- If $a = 0$ then $d = e = z = 0$, so we obtain $\lambda_2 > 0$
- If $b = 0$ we obtain $\lambda_1 > 0$ and $\lambda_3 > 0$
- If $c = 0$ and $ab = d^2 + e^2$ we obtain $\lambda_{15} + 2\sqrt{\lambda_1 \lambda_2} > 0$
- If $a = \sqrt{\lambda_2 / \lambda_1} b$ and $g = h = d = e = 0$ then $\lambda_8 + 2\sqrt{\lambda_2 \lambda_3} > 0$
- If $b = \sqrt{\lambda_3 / \lambda_2} c$, $bc = g^2 + h^2$ and $d = e = 0$ then $\lambda_8 + \lambda_7 + 2\sqrt{\lambda_2 \lambda_3} > 0$
- $\lambda_{15} + \lambda_6 + 2\sqrt{\lambda_1 \lambda_2} > 0$

These constraints are used in our numerical analysis of muon anomalous magnetic moment and dark matter.

Due to the scalar field charge assignments the mass matrix $M_{\eta\rho}^2$ is the same in both our Models 1 and 2, described in the previous sections. In the basis $\text{Re } \eta^0, \text{Re } \rho, \text{Im } \eta^0, \text{Im } \rho$ this matrix is given by:

$$M_{\eta\rho}^2 = \begin{pmatrix} m_{11} & m_{12} & 0 & 0 \\ m_{21} & m_{22} & 0 & 0 \\ 0 & 0 & m_{33} & m_{34} \\ 0 & 0 & m_{43} & m_{44} \end{pmatrix} \quad (15)$$

where the matrix entries are:

$$m_{11} = -\mu^2_\eta + \frac{1}{2}\lambda_{19}v_\xi^2 + \frac{1}{2}\lambda_{17}v_\chi^2 + \frac{1}{2}\lambda_6v_\phi^2 + \frac{1}{2}\lambda_{15}v_\phi^2, \quad (16)$$

$$m_{22} = -\mu^2_\rho + \lambda_{21}v_\xi v_\chi + \frac{1}{2}\lambda_{20}v_\xi^2 + \frac{1}{2}\lambda_{18}v_\chi^2 + \frac{1}{2}\lambda_{16}v_\phi^2, \quad (17)$$

$$m_{33} = -\mu^2_\eta + \frac{1}{2}\lambda_{19}v_\xi^2 + \frac{1}{2}\lambda_{17}v_\chi^2 + \frac{1}{2}\lambda_6v_\phi^2 + \frac{1}{2}\lambda_{15}v_\phi^2, \quad (18)$$

$$m_{44} = -\mu^2_\rho - \lambda_{21}v_\xi v_\chi + \frac{1}{2}\lambda_{20}v_\xi^2 + \frac{1}{2}\lambda_{18}v_\chi^2 + \frac{1}{2}\lambda_{16}v_\phi^2, \quad (19)$$

$$m_{12} = m_{21} = \frac{fv_\phi}{\sqrt{2}}, \quad (20)$$

$$m_{34} = m_{43} = -\frac{fv_\phi}{\sqrt{2}}. \quad (21)$$

The upper left and lower right blocks of the matrix given in Eq. (15) correspond to the squared scalar mass matrices for the dark CP even and CP odd scalars, respectively. Their diagonalization yields the following physical CP even and CP odd mass eigenstates defined as follows:

$$\begin{pmatrix} H_1 \\ H_2 \end{pmatrix} = \begin{pmatrix} \cos\theta_H & \sin\theta_H \\ -\sin\theta_H & \cos\theta_H \end{pmatrix} \begin{pmatrix} \eta_R \\ \rho_R \end{pmatrix}, \quad \begin{pmatrix} A_1 \\ A_2 \end{pmatrix} = \begin{pmatrix} \cos\theta_A & \sin\theta_A \\ -\sin\theta_A & \cos\theta_A \end{pmatrix} \begin{pmatrix} \eta_I \\ \rho_I \end{pmatrix}. \quad (22)$$

Here, $\eta_{R,I} = \text{Re } \eta^0, \text{Im } \eta^0$. These relations will be used in the analysis of the lepton mass generation, muon anomalous magnetic moment and dark matter we will carry out in the following sections.

IV. LEPTON SECTOR MASSES

Here we show that, both above specified one- and two-loop models offer radiative mechanisms for the generation of charged lepton and neutrino masses. In both models the charged lepton masses are generated at one-loop level, according to Fig. 1. On the other hand, neutrino masses arise at one- and two-loop levels depending on the model, as shown in Figs. 2, 3.

A. Charged lepton masses

From the SM charged lepton Yukawa terms in (9) and (12), we find that the mass matrix for SM charged leptons in models 1 and 2 is represented by the diagram in Fig. 1. Analytically we have

$$(M_l)_{ij} = \sum_{k=1}^3 \frac{y_{ik}^{(E)} x_{kj}^{(l)} m_{E_k}}{16\pi^2} \{ [F(m_{H_1}^2, m_{E_k}^2) - F(m_{H_2}^2, m_{E_k}^2)] \sin 2\theta_H - [F(m_{A_1}^2, m_{E_k}^2) - F(m_{A_2}^2, m_{E_k}^2)] \sin 2\theta_A \}, \quad (23)$$

where $F(m_1^2, m_2^2)$ is the function defined as,

$$F(m_1^2, m_2^2) = \frac{m_1^2}{m_1^2 - m_2^2} \ln \left(\frac{m_1^2}{m_2^2} \right). \quad (24)$$

m_{H_1} and m_{H_2} are the masses of the physical CP even scalars, whereas m_{A_1} and m_{A_2} are those of the inert pseudoscalars.

The SM charged lepton mass matrix can be parametrized as follows:

$$M_l = A_l J_E^{-1} B_l^T, \quad J_E = \begin{pmatrix} \frac{1}{16\pi^2} m_{E_1} K_E^{(1)} & 0 & 0 \\ 0 & \frac{1}{16\pi^2} m_{E_2} K_E^{(2)} & 0 \\ 0 & 0 & \frac{1}{16\pi^2} m_{E_3} K_E^{(3)} \end{pmatrix}, \quad (25)$$

where:

$$K_E^{(n)} = [F(m_{H_1}^2, m_{E_n}^2) - F(m_{H_2}^2, m_{E_n}^2)] \sin 2\theta_H - [F(m_{A_1}^2, m_{E_n}^2) - F(m_{A_2}^2, m_{E_n}^2)] \sin 2\theta_A, \quad n = 1, 2, 3$$

$$A_l = V_L^{(l)} \widetilde{M}_l^{\frac{1}{2}} J_E^{\frac{1}{2}}, \quad B_l = V_R^{(l)} \widetilde{M}_l^{\frac{1}{2}} J_E^{\frac{1}{2}}, \quad \widetilde{M}_l = \begin{pmatrix} m_e & 0 & 0 \\ 0 & m_\mu & 0 \\ 0 & 0 & m_\tau \end{pmatrix} \quad (26)$$

Thus, both models have enough parametric freedom to successfully accommodate the SM charged lepton masses. Despite the fact that the all SM charged lepton masses arise at one loop level, the hierarchy between such masses can be successfully accommodated by having some moderate hierarchy as well as a deviation from the scenario of universality of the charged lepton Yukawa couplings. It is worth mentioning that since the SM charged lepton mass matrix arises at one loop level, the effective charged lepton Yukawa couplings are proportional to a product of two other dimensionless couplings, thus implying that a moderate hierarchy in those couplings can give rise to a quadratically larger hierarchy in the effective couplings.

B. Neutrino mass matrix

From the neutrino Yukawa interactions of both radiative models described above, we find the following neutrino mass terms:

$$-\mathcal{L}_{mass}^{(\nu)} = \frac{1}{2} \begin{pmatrix} \overline{\nu}_L^C & \overline{\nu}_R & \overline{N}_R \end{pmatrix} M_\nu \begin{pmatrix} \nu_L \\ \nu_R^C \\ N_R^C \end{pmatrix} + H.c. = \varepsilon \overline{\nu}_L \nu_R + m \overline{\nu}_L N_R + M \overline{\nu}_R^C N_R + H.c. \quad (27)$$

where neutrino mass matrix M_ν is given by Eq. (1), after which we also specified lepton number assignment of the neutrino sector. As seen, the only source of lepton number violation is the m -term. In our models this submatrix is generated after spontaneous breaking of the electroweak symmetry by a VEV $\langle \phi^0 \rangle = v$ of the SM Higgs doublet ϕ , which also breaks $U(1)_L$ of lepton number symmetry of both models with the charge assignments $L(\nu_L) = L(\nu_R) = -L(N_R) = L(\phi)/2 = L(\eta)/2 = 1$. Therefore, as seen from Eqs. (9) and (12) we have

$$m_{in} = y_{in}^{(N)} \frac{v}{\sqrt{2}}, \quad i = 1, 2, 3, \quad n = 1, 2. \quad (28)$$

Since the global $U(1)_L$ is spontaneously broken by $\langle \phi^0 \rangle$, one typically expects appearance of the corresponding SM-nonsterile massless Majoron, which is phenomenologically unacceptable. Fortunately, it does not appear as a physical state. The simultaneous spontaneous breaking the SM gauge symmetry and $U(1)_L$ guaranties that the Majoron coincides with the electrically neutral CP-odd would-be-Goldstone absorbed by Z -boson. The Dirac submatrix ε is generated at one and two loops in the models of sections IIA and IIB, respectively. The corresponding Feynman diagram are shown in Figs. 2 and 3.

The submatrix ε takes the form:

$$\varepsilon_{in} \simeq \begin{cases} \sum_{j=1}^3 \sum_{k=1}^3 \frac{y_{ik}^{(E)} x_{kn}^{(\nu)} m_{E_k}}{16\pi^2} (R_C)_{1j} (R_C)_{2j} F\left(m_{H_j^\pm}^2, m_{E_k}^2\right), & \text{for the one loop model} \\ \sum_{k=1}^2 \frac{\lambda v R_{1k} R_{2k} J\left(\frac{m_\sigma^2}{m_{H_k^\pm}^2}\right)}{96\pi^2 m_S^2} \times \\ \times \left[y^{(E)} M_E (x^{(E)})^\dagger M_{\bar{E}}^T (x^{(\nu)})^T + (x^{(\nu)}) M_{\bar{E}} (x^{(E)})^* (M_E)^T (y^{(E)})^T \right], & \text{for the 2 loop model.} \end{cases} \quad (29)$$

where, for the two loop model, we have set $m_S = \max(m_{\eta^\pm}, m_{H_k^\pm}, m_\sigma)$ and we have assumed $m_{\eta^\pm} \simeq m_{H_1^\pm} \simeq m_{H_2^\pm}$ and $m_{E_i}, m_{\bar{E}_i} \ll m_{\eta^\pm}, m_{H_k^\pm} \ll m_\sigma$ ($i = 1, 2, 3$). Besides that, λ stands for the quartic scalar coupling associated with the interaction $\varepsilon_{ab} (\eta^*)^a (\phi^*)^b S_2^+ \sigma^* + h.c.$ Furthermore, under the aforementioned assumptions, the loop function for the two loop model takes the form [27, 28]:

$$J(\varkappa) = \begin{cases} 1 + \frac{3}{\pi^2} (\ln^2 \varkappa - 1), & \text{for } \varkappa \gg 1 \\ 1, & \text{for } \varkappa \rightarrow 0. \end{cases},$$

and the electrically charged scalars in the interaction and physical basis are related as:

$$\begin{aligned} \begin{pmatrix} \eta^\pm \\ S_1^\pm \\ S_2^\pm \end{pmatrix} &= R_C \begin{pmatrix} H_1^\pm \\ H_2^\pm \\ H_3^\pm \end{pmatrix}, & \text{for the one loop model,} \\ \begin{pmatrix} S_1^\pm \\ S_2^\pm \end{pmatrix} &= R \begin{pmatrix} H_1^\pm \\ H_2^\pm \end{pmatrix} = \begin{pmatrix} \cos \theta & -\sin \theta \\ \sin \theta & \cos \theta \end{pmatrix} \begin{pmatrix} H_1^\pm \\ H_2^\pm \end{pmatrix}, & \eta^\pm = H^\pm, \quad \text{for the two loop model,} \end{aligned} \quad (30)$$

where R_C is a real orthogonal 3×3 matrix.

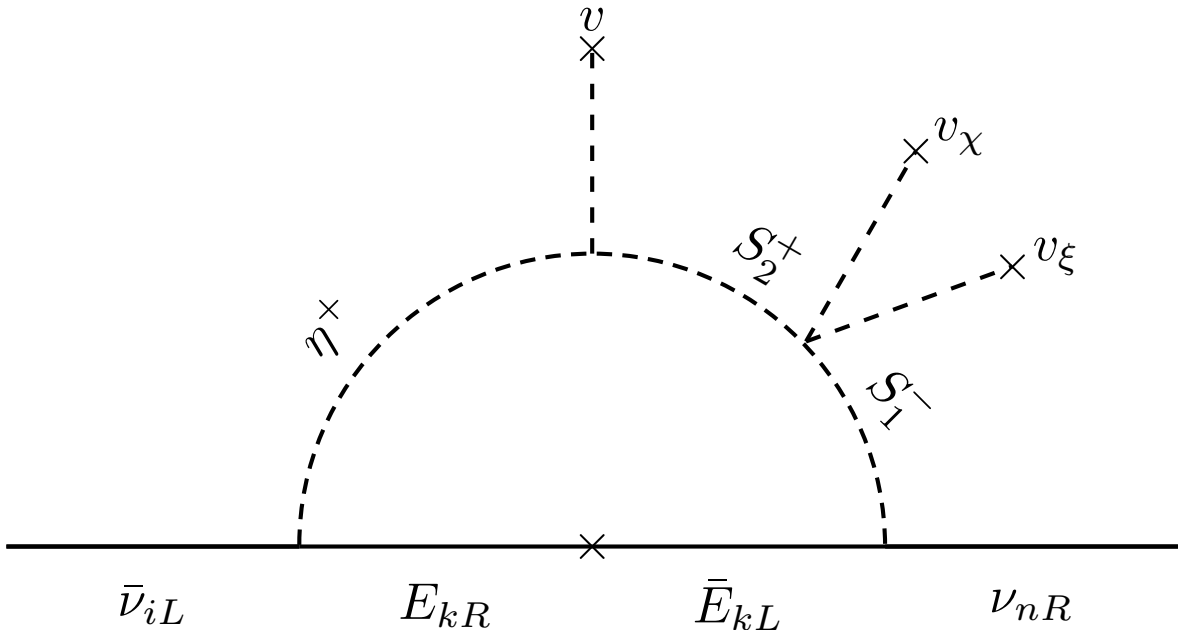


Figure 2: Model 1. One-loop Feynman diagram contributing to the neutrino mass submatrix ε . Here $i, k, r = 1, 2, 3$, $n = 1, 2$.

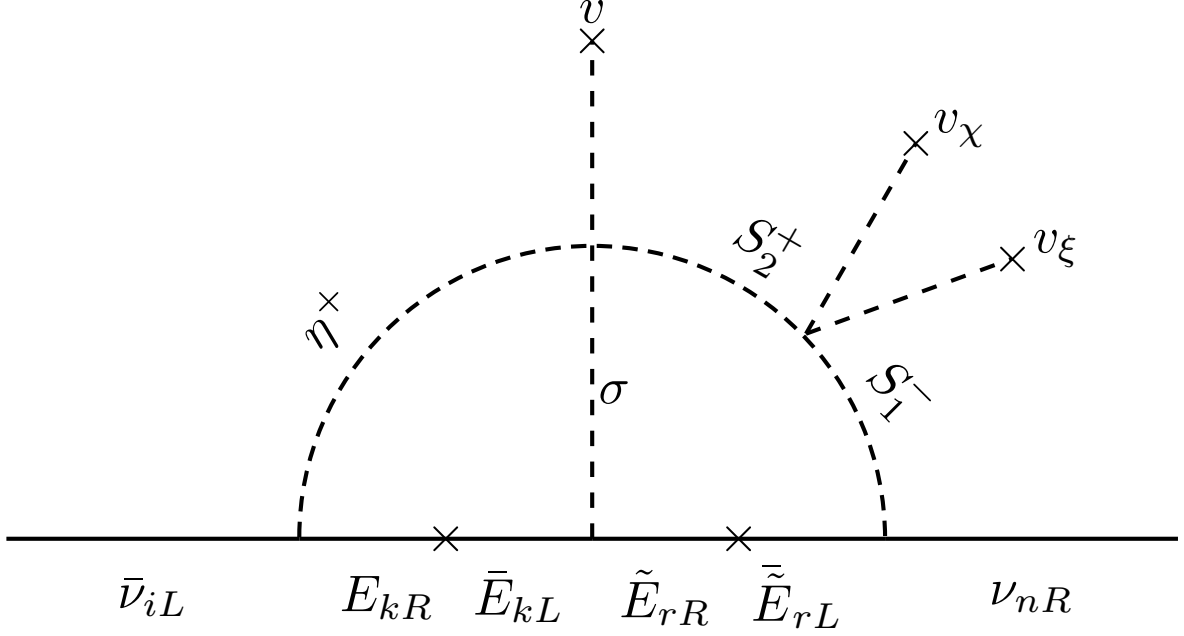


Figure 3: Model 2. Two-loop Feynman diagram contributing to the neutrino mass submatrix ε . Here $i, k, r = 1, 2, 3$, $n = 1, 2$.

From the linear seesaw mass matrix (1), (27) we have the physical neutrino mass matrices

$$M_\nu^{(1)} \cong - \left[\varepsilon M^{-1} m^T + m (M^T)^{-1} \varepsilon^T \right], \quad (31)$$

$$M_\nu^{(2)} \cong -\frac{1}{2} (M + M^T) \left[1_{2 \times 2} - (M + M^T)^{-2} m_1^T m_1 \right] - (M + M^T)^{-1} m_1^T m_1, \quad m_1 = m - \varepsilon, \quad (32)$$

$$M_\nu^{(3)} \cong \frac{1}{2} (M + M^T) \left[1_{2 \times 2} - (M + M^T)^{-2} m_2^T m_2 \right] + (M + M^T)^{-1} m_2^T m_2, \quad m_2 = m + \varepsilon, \quad (33)$$

where $M_\nu^{(1)}$ corresponds to the active neutrino mass matrix whereas $M_\nu^{(2)}$ and $M_\nu^{(3)}$ are the sterile neutrino mass matrices. The physical neutrino spectrum is composed of 3 light active neutrinos and 2 pairs of nearly degenerate sterile exotic pseudo-Dirac neutrinos N_1^\pm and N_2^\pm . For more details about diagonalization see Appendix A.

Assuming that the scalar and fermionic seesaw mediators in the diagrams Figs. 2 and 3 have masses at the scales m_S and m_E , respectively, the light active neutrino mass scale can be estimated for the one and two loop models as follows:

$$m_\nu \sim \begin{cases} \frac{\lambda y^3 v^2 f m_E}{16 \pi^2 m_S^2 M} & \text{for the one loop model} \\ \frac{\lambda^2 y^4 v^2 m_E^2}{256 \pi^4 m_S^2 M} & \text{for the two loop model.} \end{cases} \quad (34)$$

where y is a common coupling of the neutrino Yukawa interactions, whereas λ is the couplings of the quartic scalar interaction $S_1^+ S_2^- \chi \xi$, whereas f is the trilinear scalar coupling for the interaction $\eta^\dagger \phi \rho$ (see Figures 2 and 3). Assuming that $y \sim \lambda \sim \mathcal{O}(0.1)$, $f \sim m_E \sim \mathcal{O}(1)$ TeV, $m_S \sim \mathcal{O}(10)$ TeV, we find from Eq. (34) that the light active neutrino mass scale $m_\nu \sim 50$ meV can be reproduced in the one loop linear seesaw model provided that the mass scale of the heavy pseudo-Dirac neutrinos satisfies $M \sim \mathcal{O}(10^3)$ TeV. Regarding the two loop linear seesaw model, the choice $\lambda \sim \mathcal{O}(1)$, $y \sim \mathcal{O}(0.1)$, $f \sim m_E \sim \mathcal{O}(1)$ TeV, $m_S \sim \mathcal{O}(10)$ TeV allows us to reproduce the light active neutrino mass scale $m_\nu \sim 50$ meV, for pseudo-Dirac neutrinos with masses around $M \sim \mathcal{O}(1)$ TeV.

V. $g - 2$ MUON ANOMALY

The current experimental data on the anomalous dipole magnetic moment of the muon $a_\mu = (g_\mu - 2)/2$ show significant deviation from its SM value

$$\Delta a_\mu = a_\mu^{\text{exp}} - a_\mu^{\text{SM}} = (2.49 \pm 0.48) \times 10^{-9} \quad [29-34] \quad (35)$$

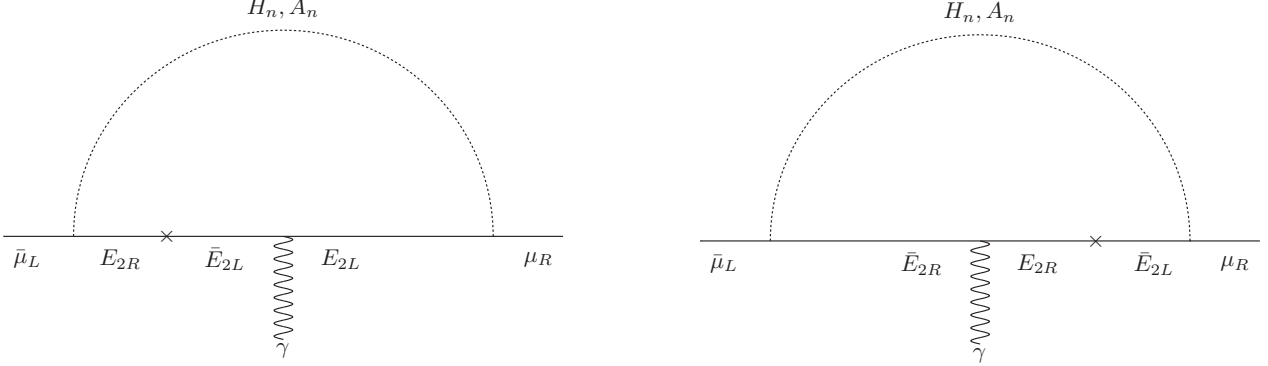


Figure 4: Loop Feynman diagrams contributing to the muon anomalous magnetic moment. Here $n = 1, 2$.

In our models this deviation is given by the sum of the partial contributions:

$$\Delta a_\mu = \sum_{i=1}^2 \sum_{\Phi=H_i, A_i} \Delta a_\mu(\Phi), \quad (36)$$

shown in Fig. 4, which involves the one loop level exchange of neutral scalars and pseudoscalars as well as charged vector-like leptons running in the internal lines of the loop. This is different than in other neutrino mass models, like the ones considered in [35–37], where the muon anomalous magnetic moment receives contributions arising from the virtual exchange of electrically charged scalars and right handed Majorana neutrinos. The analytical form for the neutral scalar and pseudoscalar contributions at one loop to Δa_μ can be found in [38–42]. Using these results we write the contributions of the neutral scalars $\Phi = H_i, A_i$ ($i = 1, 2$) defined in Eq. (22). These contributions are given by:

$$\Delta a_\mu = \frac{m_\mu^2}{8\pi^2} \left\{ \sum_{i=1}^2 \omega_{S\mu}^2 \frac{G_S^{(\mu)}(m_{E_2}, m_{H_i})}{m_{H_i}^2} + \sum_{i=1}^2 \omega_{P\mu}^2 \frac{G_P^{(\mu)}(m_{E_2}, m_{A_i})}{m_{A_i}^2} \right\} \quad (37)$$

where the loop function is given by:

$$G_{S,P}^{(l)}(m_E, m_\Phi) = \int_0^1 dx \frac{x^2(1-x \pm \epsilon_{lE})}{(1-x)(1-x\lambda_{\mu\Phi}^2) + x\epsilon_{\mu E}^2\lambda_{\mu\Phi}^2}, \quad \Phi = H_i, A_i \quad (38)$$

with $\lambda_{\mu\Phi} = m_\mu/m_\Phi$, $\epsilon_{\mu E} = m_{E_2}/m_\mu$. In the loop function $G_{S,P}$, the plus and minus signs stand for the scalar (CP-even) and pseudoscalar (CP-odd) contributions, respectively. The quantities $\omega_{S\mu}$ $\omega_{P\mu}$ are the effective Yukawa couplings for the interactions of the CP-even and CP-odd scalar fields with fermions in the form $\bar{l}_{iL}\eta E_{jR}$ and $\bar{E}_{iL}\rho l_{jR}$ after diagonalization.

The central experimental value of the muon anomalous magnetic moment shown in Eq. (35) can be successfully reproduced at the following benchmark point specified in terms of the masses of the scalars A_i, H_k and charged exotic

leptons E_n along with the effective Yukawa couplings $\omega_{S\mu(P\mu)}$:

$$m_{H_1} \approx 10164.1 \text{ GeV} \quad m_{H_2} \approx 3782.1 \text{ GeV} \quad m_{A_1} \approx 5860.1 \text{ GeV} \quad (39)$$

$$m_{A_2} \approx 3781.9 \text{ GeV} \quad m_{E_1} \approx 611.5 \text{ GeV} \quad m_{E_2} \approx 625 \text{ GeV} \quad (40)$$

$$\omega_{S\mu} \approx 1.569 \quad \omega_{P\mu} \approx 1.578 \quad (41)$$

According to Eqs. (16)-(21), this benchmark point corresponds to the model parameters

$$v_\phi = 246 \text{ GeV}, \quad v_\chi \approx 8381.8 \text{ GeV} \quad v_\xi \approx 8381.8 \text{ GeV} \quad (42)$$

$$\mu_\rho \approx 383.5 \text{ GeV} \quad \mu_\eta \approx 383.5 \text{ GeV} \quad f \approx 830 \text{ GeV} \quad (43)$$

$$\lambda_6 = \lambda_{15} = \lambda_{16} \approx 0.0970 \quad \lambda_{17} = \lambda_{19} \approx 0.205 \quad \lambda_{18} = \lambda_{20} = \lambda_{21} \approx 0.981 \quad (44)$$

VI. SCALAR DARK MATTER

As we already mentioned, a viable DM candidate in the one loop radiative linear seesaw model is the lightest among the \tilde{Z}_2 -odd scalars. Regarding the two loop linear seesaw model, due to the preserved $Z_2^{(2)} \times \tilde{Z}_2$ symmetry, one scalar DM candidate is the lightest among the Re σ and Im σ and the other one is the lightest among \tilde{Z}_2 -odd scalars. This implies that in this model we have a multicomponent dark matter and thus the resulting relic density will be the sum of the relic densities generated by these two scalar DM candidates. As to a fermionic DM candidate, this could be the lightest of the \tilde{Z}_2 -odd mass eigenstate linear combinations of ν_{nR} , N_{nR} ($n = 1, 2$) with the typical mass M specified in Eqs. (32), (33). However, it is less interesting DM candidate. In fact, as we showed in sec. IV B, the smallness of the active neutrino masses in Eq. (34) implies M to be sufficiently large. Otherwise Yukawa and quartic couplings are very small making the related phenomenology scarce, such as for example very tiny rates for charged lepton flavor violating decays. On the other hand the \tilde{Z}_2 -odd right handed neutrino states with M greater than the SM Higgs boson mass M_H are not DM candidates since they can decay into the SM Higgs boson and an active neutrino.

For these reasons we focus on the scalar DM candidates and proceed to analyze the implications of the one loop linear seesaw model in dark matter. The detailed study of the implications of the two loop linear seesaw model in dark matter is left beyond the scope of the present paper and is deferred for a future work. In the benchmark scenario (39)-(42) the DM candidate is the CP-odd scalar A_2 , defined in Eq. (22). We denote this particle as A . After diagonalizing the CP-odd scalar mass matrix in Eq. (15), we find the couplings of A to the 126 GeV SM-like Higgs boson

$$\lambda_{hhAA} = \lambda_{16} \sin^2 \theta_A + \lambda_6 \cos^2 \theta_A + \lambda_{15} \cos^2 \theta_A \quad (45)$$

$$\begin{aligned} \lambda_{hAA} = & -\sqrt{2}f \sin \theta_A \cos \theta_A + \lambda_{16} v_\phi \sin^2 \theta_A + \lambda_6 v_\phi \cos^2 \theta_A \\ & + \lambda_{15} v_\phi \cos^2 \theta_A, \end{aligned} \quad (46)$$

where, $\theta_A \approx 3.13$ is the mixing angle of the CP-odd scalar fields that was fitted with muon g-2 anomaly in Section V. For the calculation of the relic density abundance Ωh^2 of our scalar DM candidate A we specify its annihilation channels in Fig. 5. They are annihilation (a) into a pair of the SM Higgses h via quartic coupling λ_{hhAA} , (b) into a pair of the SM electroweak bosons via the gauge coupling as well as (c) into a pair the SM fermions or the SM Higgses via a Higgs-portal like diagrams consisting of the trilinear coupling λ_{hAA} and the SM Yukawa coupling or trilinear Higgs coupling. Note that due to the conservation of CP in the scalar sector of our models, there is no coannihilation of A with other scalars, in particular, with H_2 , which in the current benchmark scenario (39)-(41), is very close in mass to the mass of A .

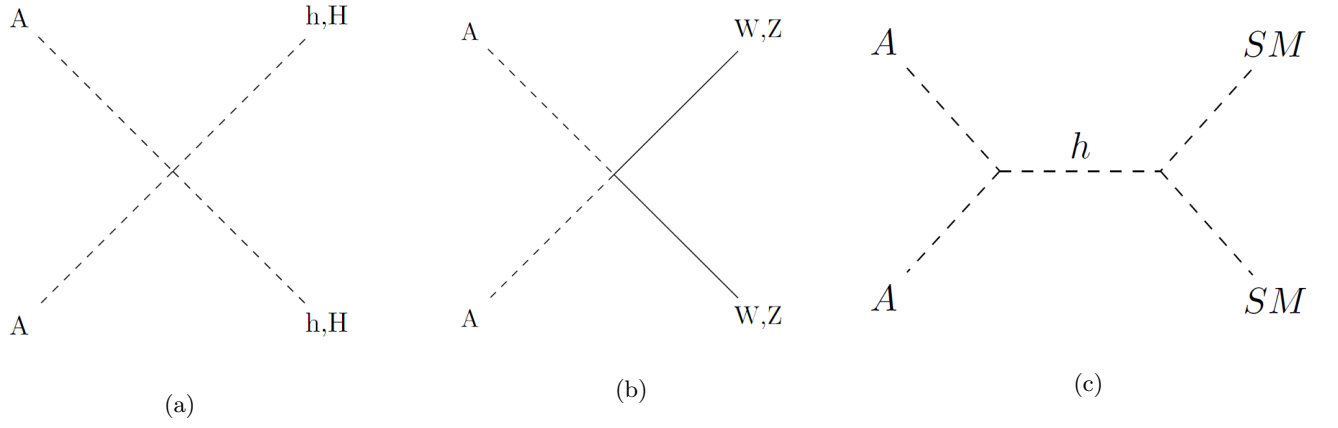


Figure 5: Relevant Feynman diagrams for DM annihilation (a), (b), (c). Here $A = A_2$ is the CP-odd scalar DM candidate and the lightest CP-even scalar $H = H_2$.

Having this at hand, we calculated DM relic abundance Ωh^2 with the help of micrOMEGAs5.2 [43] and generated a scatter plot characterizing the correlation between Ωh^2 and DM candidate mass m_{A_2} , shown in Fig. 6 for the case of the benchmark point (39)-(41).

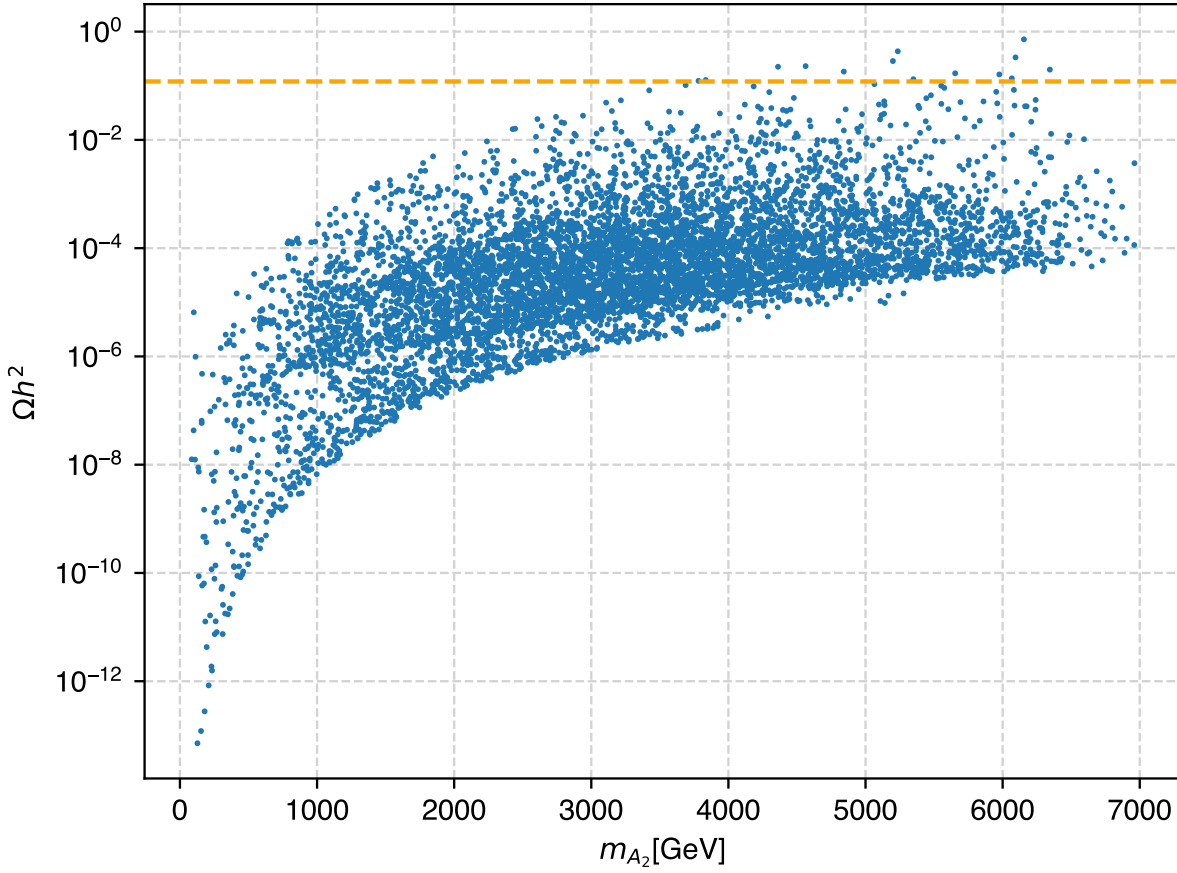


Figure 6: Correlation plot of the relic abundance Ωh^2 as a function of the DM candidate mass m_{A_2} . The orange dotted line is the experimental limit for Dark Matter relic abundance.

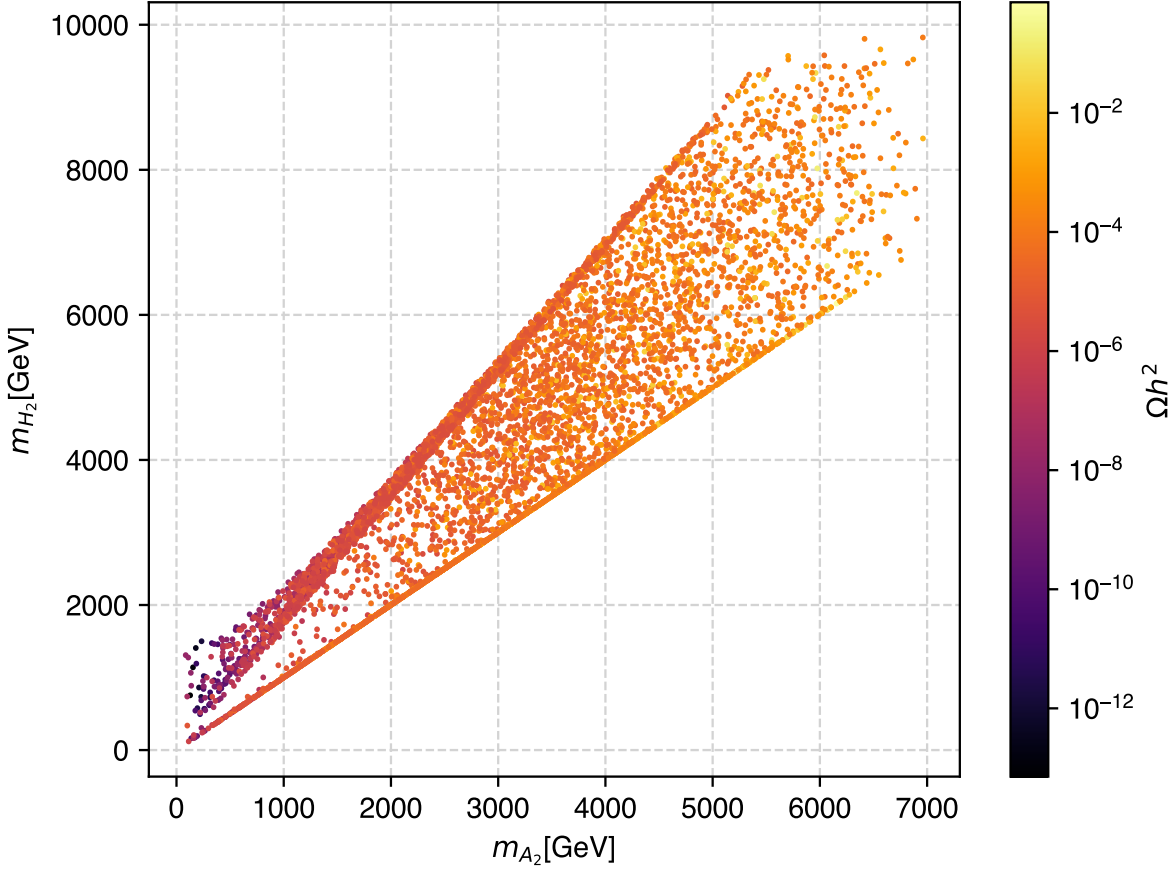


Figure 7: Correlation plot of the relic abundance Ωh^2 as a function of the DM candidate mass m_{A_2} and m_{H_2} .

The plot in Fig. 6 shows that the relic abundance is near the observed value $\Omega h^2 = 0.12 \pm 0.0012$ [44] for A_2^0 masses above 4000 GeV, and only few points are excluded by the limit. Every point in this plot fits $g - 2$ muon anomaly. The best fit values are $\Omega h^2 = 0.1231$ and $\Delta a_\mu = 2.79 \times 10^{-9}$ inside the 3σ and 1σ experimentally allowed ranges, respectively.

For completeness we studied correlations between the masses of m_{H_2} , m_{A_2} and the relic abundance Ωh^2 . The result is shown in Fig. 7. As seen, the masses of m_{H_2} and m_{A_2} are rather close and linearly correlated. Under-abundance is restricted to masses below 2 TeV. The observed relic abundance can be reached in a wide range of larger masses. We note that higher values of m_{H_2} are directly related to the values of relic abundance near the experimental limit and the values of m_{A_2} are restricted to be close to m_{H_2} .

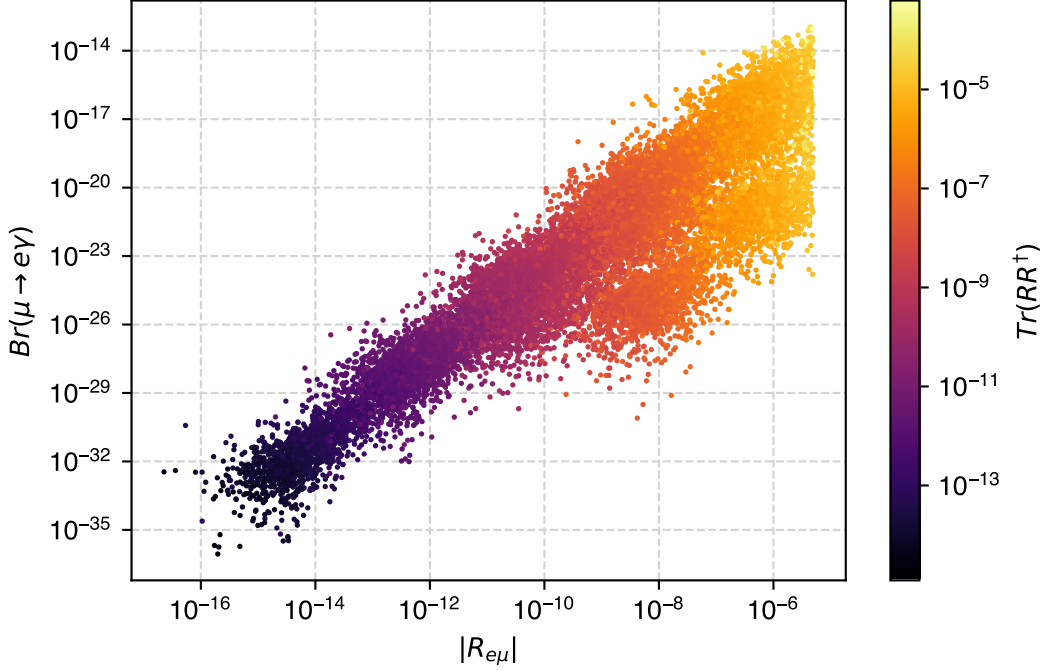


Figure 8: $\mu \rightarrow e\gamma$ branching ratio as a function of $|R_{e\mu}|$. The color surface is the value of $\text{Tr}[RR^\dagger]$.

VII. CHARGED LEPTON FLAVOR VIOLATION

In this section we analyze charged lepton flavor violation (cLFV) processes present due to the mixing between active and heavy sterile neutrinos. Here we focus on $l_i \rightarrow l_j \gamma$ decay. At one loop level its branching ratio is [45–47]

$$\text{BR}(l_i \rightarrow l_j \gamma) = \frac{\alpha_W^3 s_W^2 m_{l_i}^5}{256 \pi^2 m_W^4 \Gamma_i} |G_{ij}|^2 \quad (47)$$

$$G_{ij} \simeq \sum_{k=1}^3 \left([(1 - RR^\dagger) U_\nu]^* \right)_{ik} \left((1 - RR^\dagger) U_\nu \right)_{jk} G_\gamma \left(\frac{m_{\nu_k}^2}{m_W^2} \right) + 2 \sum_{l=1}^2 (R^*)_{il} (R)_{jl} G_\gamma \left(\frac{m_{N_{Rl}}^2}{m_W^2} \right), \quad (48)$$

$$G_\gamma(x) = \frac{10 - 43x + 78x^2 - 49x^3 + 18x^3 \ln x + 4x^4}{12(1-x)^4},$$

where $\Gamma_\mu = 3 \times 10^{-19}$ GeV is the total muon decay width, U_ν is the matrix that diagonalizes the light neutrino mass matrix which, in our case, is equal to the Pontecorvo-Maki-Nakagawa-Sakata (PMNS) matrix since the charged lepton mixing matrix is set to be equal to the identity $U_\ell = \mathbb{I}$. In addition, the matrix R is given by

$$R = \frac{1}{\sqrt{2}} m M^{-1}, \quad (49)$$

where M and m are 2×2 and 3×2 entries of 7×7 neutrino mass matrix in Eq. (1), respectively. In Fig. 8 we plot the values of the branching ratio $\text{Br}(\mu \rightarrow e\gamma)$ as a function of $|R_{e\mu}|$ for different values of $\text{Tr}[RR^\dagger]$. The points have been generated for the benchmark scenario (39)–(42) by randomly varying the neutrino mass matrix parameters (27) in the ranges $m \in [10^{-3}, 10^{-1}]$ GeV, $M \in [10, 10^3]$ GeV. According to Sec. IV B these points are compatible with the active neutrino mass scales $m_\nu \sim 50$ meV. Fig. 8 shows that there are large number of the model points below the experimental upper bound $\text{Br}(\mu \rightarrow e\gamma) < 4.2 \times 10^{-13}$ many of which should be accessible in the future experiments.

VIII. LEPTOGENESIS

Here we analyze the implications of our two-loop model for leptogenesis. We skip the one-loop model, where the Yukawa couplings responsible of the neutrino mass, discussed in Sec. IV B, are typically smaller than in the two-loop model and, as a result, its effect on leptogenesis should be smaller. To simplify our analysis we assume that M is a diagonal matrix satisfying the condition $|M_{11}| \ll |M_{22}|$. In this case the Baryon asymmetry of the Universe (BAU) is dominated in our model by N_1^\pm pseudo-Dirac sterile neutrino, defined in Sec. IV B. This situation is similar as in [48, 49] where the contribution to the baryon asymmetry arising from the remaining heavy neutral leptons is negligible. We further assume that the exotic leptonic fields E_{nR} and Ω_{nR} are heavier than the lightest pseudo-Dirac fermion $N_1^\pm = N_\pm$. We use the basis where the SM charged lepton mass matrix is diagonal. Then, the lepton asymmetry parameter, which is induced by the decay of N_\pm , has the following form [50, 51]:

$$\epsilon_\pm = \frac{\sum_{i=1}^3 \left[\Gamma(N_\pm \rightarrow \tilde{E}_i S_1^+) - \Gamma(N_\pm \rightarrow \tilde{E}_i S_1^-) \right]}{\sum_{i=1}^3 \left[\Gamma(N_\pm \rightarrow \tilde{E}_i S_1^+) + \Gamma(N_\pm \rightarrow \tilde{E}_i S_1^-) \right]} \simeq \frac{\text{Im} \left\{ \left(\left[(y_{N_+})^\dagger (y_{N_-}) \right]_{11} \right)^2 \right\}}{8\pi A_\pm} \frac{r}{r^2 + \frac{\Gamma_\pm^2}{m_{N_\pm}^2}}, \quad (50)$$

with:

$$\begin{aligned} r &= \frac{m_{N_+}^2 - m_{N_-}^2}{m_{N_+} m_{N_-}}, & A_\pm &= \left[(y_{N_\pm})^\dagger y_{N_\pm} \right]_{11}, & \Gamma_\pm &= \frac{A_\pm m_{N_\pm}}{8\pi}, \\ y_{N_+} &= \frac{x^{(\nu)}}{\sqrt{2}} \left(1_{2 \times 2} - \frac{1}{2} B_2^T B_2 - B_1^T B_2 \right), \\ y_{N_-} &= \frac{x^{(\nu)}}{\sqrt{2}} \left(1_{2 \times 2} - \frac{1}{2} B_1^T B_1 \right), \\ B_1 &\simeq -\sqrt{2} m_2 (M + M^T)^{-1} \simeq -\frac{1}{\sqrt{2}} m_2 M^{-1} = -\frac{1}{\sqrt{2}} (m - \varepsilon) M^{-1}, \\ B_2 &\simeq -\sqrt{2} m_1 (M + M^T)^{-1} \simeq -\frac{1}{\sqrt{2}} m_1 M^{-1} = -\frac{1}{\sqrt{2}} (m + \varepsilon) M^{-1}. \end{aligned} \quad (51)$$

As mentioned in [52], neglecting the interference terms involving the two different sterile neutrinos N_\pm leads to huge values of the washout parameter $K_{N_+} + K_{N_-}$. Thus, this effect must be taken into account. The small mass splitting in the pair of the states N_\pm , forming a pseudo-Dirac neutrino, leads to destructive interference in the scattering process [53] properly reducing the washout parameter. Its effective value, including the interference term, is given by

$$K^{eff} \simeq (K_{N_+} \delta_+^2 + K_{N_-} \delta_-^2), \quad (52)$$

where:

$$\delta_\pm = \frac{m_{N_+} - m_{N_-}}{\Gamma_{N_\pm}}, \quad K_{N_\pm} = \frac{\Gamma_\pm}{H(T)}, \quad H(T) = \sqrt{\frac{4\pi^3 g^*}{45}} \frac{T^2}{M_P} \quad (53)$$

where $g^* = 106.75$ is the number of effective relativistic degrees of freedom, $M_{Pl} = 1.2 \times 10^9$ GeV is the Planck constant and $T = m_{N_\pm}$. In the weak and strong washout regimes, the baryon asymmetry is related to the lepton asymmetry [51] as follows

$$Y_{\Delta B} = \frac{n_B - \bar{n}_B}{s} = -\frac{28}{79} \frac{\epsilon_+ + \epsilon_-}{g^*}, \quad \text{for } K^{eff} \ll 1, \quad (54)$$

$$Y_{\Delta B} = \frac{n_B - \bar{n}_B}{s} = -\frac{28}{79} \frac{0.3(\epsilon_+ + \epsilon_-)}{g^* K^{eff} (\ln K^{eff})^{0.6}}, \quad \text{for } K^{eff} \gg 1, \quad (55)$$

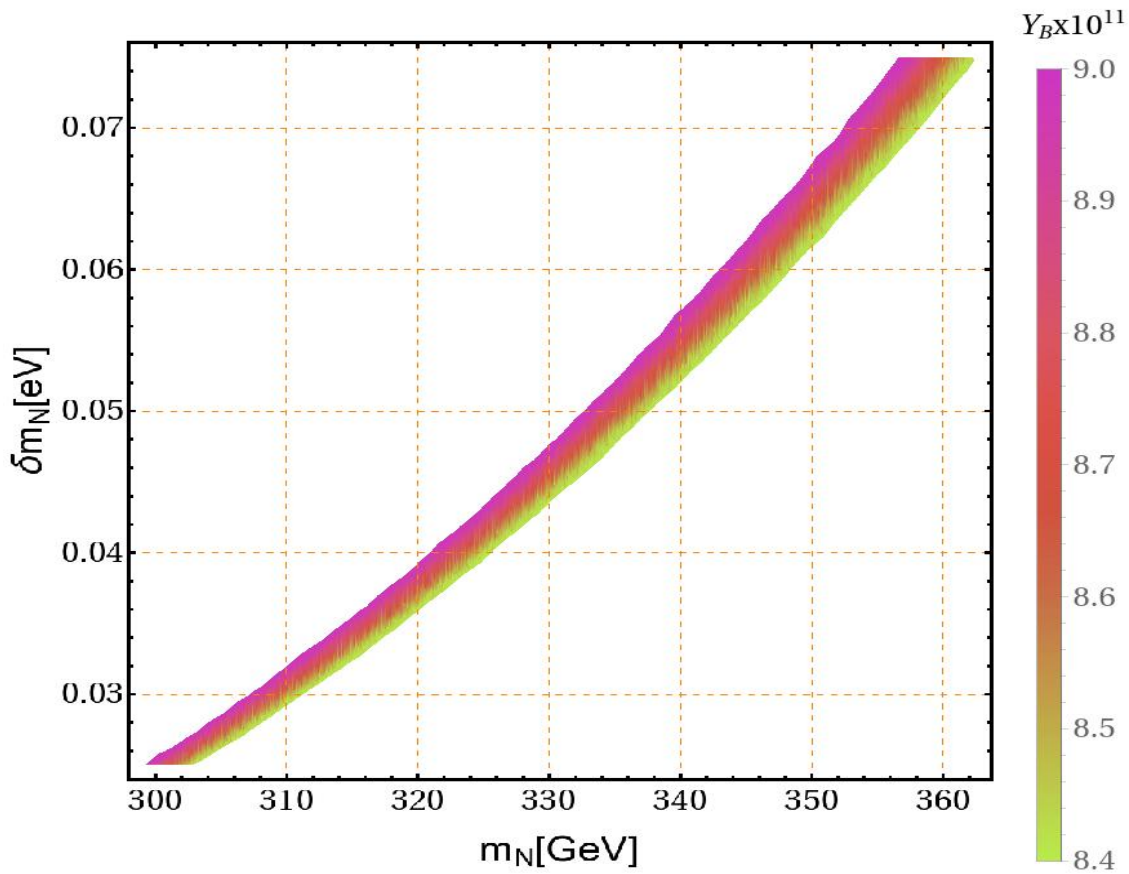


Figure 9: Correlation of the sterile neutrino mass splitting δm_N with the mass of the lightest sterile neutrino for the weak washout regime.

The correlation of the sterile neutrino mass splitting δm_N with the mass of the lightest sterile neutrino for the weak washout regime is shown in Figure 9. To generate this plot, we performed a random scan in the ranges $(m_{\nu D})_{ij} \in [1, 150]$ GeV, $M_{11} \in [150, 500]$ GeV, $M_{22} \in [1, 2]$ TeV and $\delta m_N \in [0.5, 1.5]$ eV. As indicated by Figure 9, an increase of the sterile neutrino mass splitting δm_N yields larger values for the mass m_N of the lightest pseudo-Dirac lepton, in order to successfully reproduce the observed value of the baryon asymmetry [54]

$$Y_{\Delta B} = \frac{n_B - n_{\bar{B}}}{s} = (0.87 \pm 0.01) \times 10^{-10} \quad (56)$$

Such larger values of the lightest pseudo-Dirac lepton mass m_N will give rise to smaller active-sterile neutrino mixing angles, thus yielding smaller rates for charged lepton flavor violating decays such as $\mu \rightarrow e\gamma$. As shown by Figure 9, our model is capable of successfully accommodating the baryon asymmetry of the Universe via resonant leptogenesis.

IX. CONCLUSIONS

We have proposed two models where the tiny masses of the light active neutrinos are generated from a radiative linear seesaw mechanism, with the Dirac neutrino mass submatrix arising at one and two loop levels in the first and second model, respectively, due to the virtual electrically charged scalars and vector-like leptons running inside the loops. In these models, the masses of the SM charged leptons are generated from a one loop radiative seesaw mechanism, mediated by charged exotic vector like leptons and electrically neutral scalars. This loop pattern, engendering small

masses to the light active neutrinos and the SM charged lepton masses, is ensured by a preserved \tilde{Z}_2 discrete symmetry, which also guarantees stability of the scalar dark matter candidate in our models. These models can be treated as extended Inert Doublet Models (IDM), where the scalar content is augmented with the inclusion of several electrically neutral and electrically charged scalar singlets, whereas the lepton sector is enlarged with right handed Majorana neutrinos and charged exotic vector like leptons. We have found that these models can successfully comply with the constraints arising from charged lepton flavor violation, leptogenesis, dark matter and muon anomalous magnetic moment.

Comment

Our friend and collaborator Iván Schmidt passed away during the completion of this work. He will be sorely missed.

Acknowledgments

A.E.C.H, I.S, S.K and N.P are supported by ANID-Chile FONDECYT 1210378, ANID-Chile FONDECYT 1180232, ANID-Chile FONDECYT 3150472, ANID-Chile FONDECYT 1230160, ANID PIA/APOYO AFB230003, Milenio-ANID-ICN2019_044, ANID-Chile Doctorado Nacional año 2022 21221396 and Programa de Incentivo a la Investigación Científica (PIIC) from UTFSM.

Appendix A: Diagonalization of the neutrino mass matrix.

Here, for the convenience of the reader, we show in full detail the perturbative diagonalization procedure of the full 7×7 neutrino mass matrix M_ν of Eq. (1). The elements of the submatrices ε , m and M obey the following hierarchy:

$$\varepsilon_{in} \ll m_{in} \ll M_{np}, \quad i = 1, 2, 3, \quad n, p = 1, 2. \quad (\text{A1})$$

We start by applying the following first orthogonal transformation to the matrix M_ν :

$$\begin{aligned} S_\nu^T M_\nu S_\nu &= \begin{pmatrix} 1_{3 \times 3} & 0_{3 \times 2} & 0_{3 \times 2} \\ 0_{2 \times 3} & \frac{1}{\sqrt{2}} 1_{2 \times 2} & -\frac{1}{\sqrt{2}} 1_{2 \times 2} \\ 0_{2 \times 3} & \frac{1}{\sqrt{2}} 1_{2 \times 2} & \frac{1}{\sqrt{2}} 1_{2 \times 2} \end{pmatrix} \begin{pmatrix} 0_{3 \times 3} & \varepsilon & m \\ \varepsilon^T & 0_{2 \times 2} & M \\ m^T & M^T & 0_{2 \times 2} \end{pmatrix} \begin{pmatrix} 1_{3 \times 3} & 0_{3 \times 2} & 0_{3 \times 2} \\ 0_{2 \times 3} & \frac{1}{\sqrt{2}} 1_{2 \times 2} & \frac{1}{\sqrt{2}} 1_{2 \times 2} \\ 0_{2 \times 3} & -\frac{1}{\sqrt{2}} 1_{2 \times 2} & \frac{1}{\sqrt{2}} 1_{2 \times 2} \end{pmatrix} \\ &= \begin{pmatrix} 1_{3 \times 3} & 0_{3 \times 2} & 0_{3 \times 2} \\ 0_{2 \times 3} & \frac{1}{\sqrt{2}} 1_{2 \times 2} & -\frac{1}{\sqrt{2}} 1_{2 \times 2} \\ 0_{2 \times 3} & \frac{1}{\sqrt{2}} 1_{2 \times 2} & \frac{1}{\sqrt{2}} 1_{2 \times 2} \end{pmatrix} \begin{pmatrix} 0_{3 \times 3} & -\frac{1}{\sqrt{2}}(m - \varepsilon) & \frac{1}{\sqrt{2}}(m + \varepsilon) \\ \varepsilon^T & -\frac{1}{\sqrt{2}}M & \frac{1}{\sqrt{2}}M \\ m^T & \frac{1}{\sqrt{2}}M^T & \frac{1}{\sqrt{2}}M^T \end{pmatrix} \\ &= \begin{pmatrix} 0_{3 \times 3} & -\frac{1}{\sqrt{2}}(m - \varepsilon) & \frac{1}{\sqrt{2}}(m + \varepsilon) \\ \frac{1}{\sqrt{2}}(\varepsilon^T - m^T) & -\frac{1}{2}(M + M^T) & \frac{1}{2}M - \frac{1}{2}M^T \\ \frac{1}{\sqrt{2}}(\varepsilon^T + m^T) & \frac{1}{2}M^T - \frac{1}{2}M & \frac{1}{2}(M + M^T) \end{pmatrix} \\ &\cong \begin{pmatrix} 0_{3 \times 3} & -\frac{1}{\sqrt{2}}m_1 & \frac{1}{\sqrt{2}}m_2 \\ -\frac{1}{\sqrt{2}}m_1^T & -\frac{1}{2}(M + M^T) & 0_{2 \times 2} \\ \frac{1}{\sqrt{2}}m_2^T & 0_{2 \times 2} & \frac{1}{2}(M + M^T) \end{pmatrix} \end{aligned} \quad (\text{A2})$$

where the rotation matrix S_ν is given by:

$$S_\nu = \begin{pmatrix} 1_{3 \times 3} & 0_{3 \times 2} & 0_{3 \times 2} \\ 0_{2 \times 3} & \frac{1}{\sqrt{2}} 1_{2 \times 2} & \frac{1}{\sqrt{2}} 1_{2 \times 2} \\ 0_{2 \times 3} & -\frac{1}{\sqrt{2}} 1_{2 \times 2} & \frac{1}{\sqrt{2}} 1_{2 \times 2} \end{pmatrix}, \quad (\text{A3})$$

and the submatrices m_1 and m_2 have the form:

$$m_1 = m - \varepsilon, \quad m_2 = m + \varepsilon. \quad (\text{A4})$$

Now we perform a second orthogonal transformation under the matrix M_ν as follows:

$$\begin{aligned} & R_{1\nu}^T S_\nu^T M_\nu S_\nu R_{1\nu} \quad (\text{A5}) \\ &= \begin{pmatrix} 1_{3 \times 3} - \frac{1}{2} B_1 B_1^T & 0_{3 \times 2} & B_1 \\ 0_{2 \times 3} & 1_{2 \times 2} & 0 \\ -B_1^T & 0 & 1_{2 \times 2} - \frac{1}{2} B_1^T B_1 \end{pmatrix} \begin{pmatrix} 0_{3 \times 3} & -\frac{1}{\sqrt{2}} m_1 & \frac{1}{\sqrt{2}} m_2 \\ -\frac{1}{\sqrt{2}} m_1^T & -\frac{1}{2} (M + M^T) & 0_{2 \times 2} \\ \frac{1}{\sqrt{2}} m_2^T & 0_{2 \times 2} & \frac{1}{2} (M + M^T) \end{pmatrix} \\ &\quad \times \begin{pmatrix} 1_{3 \times 3} - \frac{1}{2} B_1 B_1^T & 0_{3 \times 2} & -B_1 \\ 0_{2 \times 3} & 1_{2 \times 2} & 0_{2 \times 2} \\ B_1^T & 0_{2 \times 2} & 1_{2 \times 2} - \frac{1}{2} B_1^T B_1 \end{pmatrix} \\ &= \begin{pmatrix} 1_{3 \times 3} - \frac{1}{2} B_1 B_1^T & 0_{3 \times 2} & B_1 \\ 0_{2 \times 3} & 1_{2 \times 2} & 0_{2 \times 2} \\ -B_1^T & 0_{2 \times 2} & 1_{2 \times 2} - \frac{1}{2} B_1^T B_1 \end{pmatrix} \begin{pmatrix} \frac{1}{\sqrt{2}} m_2 B_1^T & -\frac{1}{\sqrt{2}} m_1 & \frac{1}{\sqrt{2}} m_2 \\ -\frac{1}{\sqrt{2}} m_1^T & -\frac{1}{2} (M + M^T) & \frac{1}{\sqrt{2}} m_1^T B_1 \\ \frac{1}{\sqrt{2}} m_2^T + \frac{1}{2} (M + M^T) B_1^T & 0_{2 \times 2} & \frac{1}{2} (M + M^T) \end{pmatrix} \\ &\simeq \begin{pmatrix} \frac{1}{\sqrt{2}} m_2 B_1^T + B_1 \left(\frac{1}{\sqrt{2}} m_2^T + \frac{1}{2} (M + M^T) B_1^T \right) & -\frac{1}{\sqrt{2}} m_1 & \frac{1}{\sqrt{2}} m_2 + \frac{1}{2} B_1 (M + M^T) \\ -\frac{1}{\sqrt{2}} m_1^T & -\frac{1}{2} (M + M^T) & \frac{1}{\sqrt{2}} m_1^T B_1 \\ \frac{1}{\sqrt{2}} m_2^T + \frac{1}{2} (M + M^T) B_1^T & \frac{1}{\sqrt{2}} B_1^T m_1 & \frac{1}{2} (1_{2 \times 2} - \frac{1}{2} B_1^T B_1) (M + M^T) - \frac{1}{\sqrt{2}} B_1^T m_2 \end{pmatrix} \end{aligned}$$

By imposing the partial diagonalization condition:

$$(R_{1\nu}^T S_\nu^T M_\nu S_\nu R_{1\nu})_{in} = (R_{1\nu}^T S_\nu^T M_\nu S_\nu R_{1\nu})_{ni} = 0, \quad i = 1, 2, 3, \quad n = 1, 2. \quad (\text{A6})$$

we find the following relation:

$$B_1 \simeq -\sqrt{2} m_2 (M + M^T)^{-1} \quad (\text{A7})$$

which implies that:

$$\begin{aligned} & R_{1\nu}^T S_\nu^T M_\nu S_\nu R_{1\nu} \\ &\simeq \begin{pmatrix} -m_2 (M + M^T)^{-1} m_2^T & -\frac{1}{\sqrt{2}} m_1 & 0_{3 \times 2} \\ -\frac{1}{\sqrt{2}} m_1^T & -\frac{M+M^T}{2} & 0_{2 \times 2} \\ 0_{2 \times 3} & 0_{2 \times 2} & \left[1_{2 \times 2} - (M + M^T)^{-1} m_2^T m_2 (M + M^T)^{-1} \right] \frac{(M+M^T)}{2} + (M + M^T)^{-1} m_2^T m_2 \end{pmatrix} \\ &= \begin{pmatrix} -m_2 (M + M^T)^{-1} m_2^T & -\frac{1}{\sqrt{2}} m_1 & 0_{3 \times 2} \\ -\frac{1}{\sqrt{2}} m_1^T & X & 0_{2 \times 2} \\ 0_{2 \times 3} & 0_{2 \times 2} & Y \end{pmatrix} \quad (\text{A8}) \end{aligned}$$

where X and Y are given by:

$$\begin{aligned} X &= -\frac{1}{2}(M + M^T), \\ Y &= \frac{1}{2}\left[1_{2 \times 2} - (M + M^T)^{-1} m_2^T m_2 (M + M^T)^{-1}\right] (M + M^T) + (M + M^T)^{-1} m_2^T m_2, \end{aligned} \quad (\text{A9})$$

Next, we proceed to apply a third orthogonal transformation obtaining the following relation:

$$\begin{aligned} & R_{2\nu}^T R_{1\nu}^T S_\nu^T M_\nu S_\nu R_{1\nu} R_{2\nu} \\ &= \begin{pmatrix} 1_{3 \times 3} - \frac{1}{2} B_2 B_2^T & B_2 & 0_{3 \times 2} \\ -B_2^T & 1_{2 \times 2} - \frac{1}{2} B_2^T B_2 & 0_{2 \times 2} \\ 0_{2 \times 3} & 0_{2 \times 2} & 1_{2 \times 2} \end{pmatrix} \begin{pmatrix} -m_2 (M + M^T)^{-1} m_2^T & -\frac{1}{\sqrt{2}} m_1 & 0_{3 \times 2} \\ -\frac{1}{\sqrt{2}} m_1^T & X & 0_{2 \times 2} \\ 0_{2 \times 3} & 0_{2 \times 2} & Y \end{pmatrix} \\ &\times \begin{pmatrix} 1 - \frac{1}{2} B_2 B_2^T & -B_2 & 0_{3 \times 2} \\ B_2^T & 1_{2 \times 2} - \frac{1}{2} B_2^T B_2 & 0_{2 \times 2} \\ 0_{2 \times 3} & 0_{2 \times 2} & 1_{2 \times 2} \end{pmatrix} \\ &\simeq \begin{pmatrix} 1_{3 \times 3} - \frac{1}{2} B_2 B_2^T & B_2 & 0_{3 \times 2} \\ -B_2^T & 1_{2 \times 2} - \frac{1}{2} B_2^T B_2 & 0_{2 \times 2} \\ 0_{2 \times 3} & 0_{2 \times 2} & 1_{2 \times 2} \end{pmatrix} \begin{pmatrix} -m_2 (M + M^T)^{-1} m_2^T - \frac{1}{\sqrt{2}} m_1 B_2^T & -\frac{1}{\sqrt{2}} m_1 & 0_{3 \times 2} \\ -\frac{1}{\sqrt{2}} m_1^T + X B_2^T & X & 0_{2 \times 2} \\ 0_{2 \times 3} & 0_{2 \times 2} & Y \end{pmatrix} \\ &\simeq \begin{pmatrix} -m_2 (M + M^T)^{-1} m_2^T - \frac{1}{\sqrt{2}} m_1 B_2^T - \frac{1}{\sqrt{2}} B_2 m_1^T + B_2 X B_2^T & -\frac{1}{\sqrt{2}} m_1 + B_2 X & 0_{3 \times 2} \\ -\frac{1}{\sqrt{2}} m_1^T + X B_2^T & X (1_{2 \times 2} - \frac{1}{2} B_2^T B_2) + \frac{1}{\sqrt{2}} B_2^T m_1 & 0_{2 \times 2} \\ 0_{2 \times 3} & 0_{2 \times 2} & Y \end{pmatrix} \end{aligned} \quad (\text{A10})$$

The partial diagonalization condition yields the relation:

$$(R_{2\nu}^T R_{1\nu}^T S_\nu^T M_\nu S_\nu R_{1\nu} R_{2\nu})_{in} = (R_{2\nu}^T R_{1\nu}^T S_\nu^T M_\nu S_\nu R_{1\nu} R_{2\nu})_{ni} = 0, \quad i = 1, 2, 3, \quad n = 1, 2. \quad (\text{A11})$$

then implying the relation:

$$B_2 \simeq \frac{1}{\sqrt{2}} m_1 X^{-1} \simeq -\sqrt{2} m_1 (M + M^T)^{-1}. \quad (\text{A12})$$

Thus, the 7×7 neutrino mass matrix M_ν of Eq. (1) can be block diagonalized as follows:

$$R_{2\nu}^T R_{1\nu}^T S_\nu^T M_\nu S_\nu R_{1\nu} R_{2\nu} \simeq \begin{pmatrix} M_\nu^{(1)} & 0_{3 \times 2} & 0_{3 \times 2} \\ 0_{2 \times 3} & M_\nu^{(2)} & 0_{2 \times 2} \\ 0_{2 \times 3} & 0_{2 \times 2} & M_\nu^{(3)} \end{pmatrix}, \quad (\text{A13})$$

where $M_\nu^{(1)}$ is the mass matrix for light active neutrinos, whereas $M_\nu^{(2)}$ and $M_\nu^{(3)}$ are the sterile neutrino mass matrices. These matrices are given by:

$$\begin{aligned} M_\nu^{(1)} &\simeq -m_2 (M + M^T)^{-1} m_2^T - \frac{1}{\sqrt{2}} m_1 B_2^T - \frac{1}{\sqrt{2}} B_2 m_1^T + B_2 X B_2^T \\ &\simeq -m_2 (M + M^T)^{-1} m_2^T + m_1 (M + M^T)^{-1} m_1^T + m_1 (M + M^T)^{-1} m_1^T - m_1 (M + M^T)^{-1} m_1^T \\ &\simeq -\left[\varepsilon M^{-1} m^T + m (M^T)^{-1} \varepsilon^T\right], \end{aligned} \quad (\text{A14})$$

$$\begin{aligned}
M_\nu^{(2)} &\simeq -\frac{1}{2} \left(1_{2 \times 2} - \frac{1}{2} B_2^T B_2 \right) (M + M^T) + \frac{1}{\sqrt{2}} B_2^T m_1 \\
&\simeq -\frac{1}{2} \left[1_{2 \times 2} - (M + M^T)^{-1} m_1^T m_1 (M + M^T)^{-1} \right] (M + M^T) - (M + M^T)^{-1} m_1^T m_1
\end{aligned} \tag{A15}$$

$$\begin{aligned}
M_\nu^{(3)} &\simeq \frac{1}{2} \left(1_{2 \times 2} - \frac{1}{2} B_1^T B_1 \right) (M + M^T) - \frac{1}{\sqrt{2}} B_1^T m_2 \\
&\simeq \frac{1}{2} \left[1_{2 \times 2} - (M + M^T)^{-1} m_2^T m_2 (M + M^T)^{-1} \right] (M + M^T) + (M + M^T)^{-1} m_2^T m_2
\end{aligned} \tag{A16}$$

where:

$$B_1 \simeq -\sqrt{2} m_2 (M + M^T)^{-1} \simeq -\frac{1}{\sqrt{2}} m_2 M^{-1} = -\frac{1}{\sqrt{2}} (m - \varepsilon) M^{-1}, \tag{A17}$$

$$B_2 \simeq -\sqrt{2} m_1 (M + M^T)^{-1} \simeq -\frac{1}{\sqrt{2}} m_1 M^{-1} = -\frac{1}{\sqrt{2}} (m + \varepsilon) M^{-1}. \tag{A18}$$

Thus, the rotation matrix R_ν that diagonalizes the full 7×7 neutrino mass matrix M_ν of Eq. (1) has the form:

$$\begin{aligned}
R_\nu &= S_\nu R_{1\nu} R_{2\nu} V_\nu \\
&\simeq \begin{pmatrix} 1_{3 \times 3} & 0_{3 \times 2} & 0_{3 \times 2} \\ 0_{2 \times 3} & \frac{1}{\sqrt{2}} 1_{2 \times 2} & \frac{1}{\sqrt{2}} 1_{2 \times 2} \\ 0_{2 \times 3} & -\frac{1}{\sqrt{2}} 1_{2 \times 2} & \frac{1}{\sqrt{2}} 1_{2 \times 2} \end{pmatrix} \begin{pmatrix} 1_{3 \times 3} - \frac{1}{2} B_1 B_1^T & 0_{3 \times 2} & -B_1 \\ 0_{2 \times 3} & 1_{2 \times 2} & 0_{2 \times 2} \\ B_1^T & 0_{2 \times 2} & 1_{2 \times 2} - \frac{1}{2} B_1^T B_1 \end{pmatrix} \\
&\times \begin{pmatrix} 1_{3 \times 3} - \frac{1}{2} B_2 B_2^T & -B_2 & 0_{3 \times 2} \\ B_2^T & 1_{2 \times 2} - \frac{1}{2} B_2^T B_2 & 0_{2 \times 2} \\ 0_{2 \times 3} & 0_{2 \times 2} & 1 \end{pmatrix} \begin{pmatrix} R_\nu^{(1)} & 0_{3 \times 2} & 0_{3 \times 2} \\ 0_{2 \times 3} & R_\nu^{(2)} & 0_{2 \times 2} \\ 0_{2 \times 3} & 0_{2 \times 2} & R_\nu^{(3)} \end{pmatrix},
\end{aligned} \tag{A20}$$

where:

$$V_\nu = \begin{pmatrix} R_\nu^{(1)} & 0_{3 \times 2} & 0_{3 \times 2} \\ 0_{2 \times 3} & R_\nu^{(2)} & 0_{2 \times 2} \\ 0_{2 \times 3} & 0_{2 \times 2} & R_\nu^{(3)} \end{pmatrix}, \tag{A21}$$

being $R_\nu^{(1)}$, $R_\nu^{(2)}$ and $R_\nu^{(3)}$ are the rotation matrices that diagonalize $M_\nu^{(1)}$, $M_\nu^{(2)}$ and $M_\nu^{(3)}$, respectively. The rotation mass matrix R_ν given above, can be rewritten as follows:

$$\begin{aligned}
R_\nu &= S_\nu R_{1\nu} R_{2\nu} V_\nu \\
&\simeq \begin{pmatrix} 1_{3\times 3} & 0_{3\times 2} & 0_{3\times 2} \\ 0_{2\times 3} & \frac{1}{\sqrt{2}} 1_{2\times 2} & \frac{1}{\sqrt{2}} 1_{2\times 2} \\ 0_{2\times 3} & -\frac{1}{\sqrt{2}} 1_{2\times 2} & \frac{1}{\sqrt{2}} 1_{2\times 2} \end{pmatrix} \begin{pmatrix} (1_{3\times 3} - \frac{1}{2} B_1 B_1^T) (1_{3\times 3} - \frac{1}{2} B_2 B_2^T) & - (1_{3\times 3} - \frac{1}{2} B_1 B_1^T) B_2 & -B_1 \\ & B_2^T & 1_{2\times 2} - \frac{1}{2} B_2^T B_2 & 0_{2\times 2} \\ & B_1^T (1_{3\times 3} - \frac{1}{2} B_2 B_2^T) & -B_1^T B_2 & 1_{2\times 2} - \frac{1}{2} B_1^T B_1 \end{pmatrix} \\
&\quad \times \begin{pmatrix} R_\nu^{(1)} & 0_{3\times 2} & 0_{3\times 2} \\ 0_{2\times 3} & R_\nu^{(2)} & 0_{2\times 2} \\ 0_{2\times 3} & 0_{2\times 2} & R_\nu^{(3)} \end{pmatrix} \\
&\simeq \begin{pmatrix} (1_{3\times 3} - \frac{1}{2} B_1 B_1^T) (1_{3\times 3} - \frac{1}{2} B_2 B_2^T) & - (1_{3\times 3} - \frac{1}{2} B_1 B_1^T) B_2 & -B_1 \\ & \frac{B_1^T + B_2^T}{\sqrt{2}} & \frac{1}{\sqrt{2}} (1_{2\times 2} - \frac{1}{2} B_2^T B_2 - B_1^T B_2) & \frac{1}{\sqrt{2}} (1_{2\times 2} - \frac{1}{2} B_1^T B_1) \\ & \frac{B_1^T - B_2^T}{\sqrt{2}} & -\frac{1}{\sqrt{2}} (1_{2\times 2} - \frac{1}{2} B_2^T B_2 + B_1^T B_2) & \frac{1}{\sqrt{2}} (1_{2\times 2} - \frac{1}{2} B_1^T B_1) \end{pmatrix} \begin{pmatrix} R_\nu^{(1)} & 0_{3\times 2} & 0_{3\times 2} \\ 0_{2\times 3} & R_\nu^{(2)} & 0_{2\times 2} \\ 0_{2\times 3} & 0_{2\times 2} & R_\nu^{(3)} \end{pmatrix} \\
&\simeq \begin{pmatrix} 1_{3\times 3} & -B_2 & -B_1 \\ \frac{B_1^T + B_2^T}{\sqrt{2}} & \frac{1}{\sqrt{2}} (1_{2\times 2} - \frac{1}{2} B_2^T B_2 - B_1^T B_2) & \frac{1}{\sqrt{2}} (1_{2\times 2} - \frac{1}{2} B_1^T B_1) \\ \frac{B_1^T - B_2^T}{\sqrt{2}} & -\frac{1}{\sqrt{2}} (1_{2\times 2} - \frac{1}{2} B_2^T B_2 + B_1^T B_2) & \frac{1}{\sqrt{2}} (1_{2\times 2} - \frac{1}{2} B_1^T B_1) \end{pmatrix} \begin{pmatrix} R_\nu^{(1)} & 0_{3\times 2} & 0_{3\times 2} \\ 0_{2\times 3} & R_\nu^{(2)} & 0_{2\times 2} \\ 0_{2\times 3} & 0_{2\times 2} & R_\nu^{(3)} \end{pmatrix} \\
&\simeq \begin{pmatrix} R_\nu^{(1)} & -B_2 R_\nu^{(2)} & -B_1 R_\nu^{(3)} \\ \frac{B_1^T + B_2^T}{\sqrt{2}} R_\nu^{(1)} & \frac{1}{\sqrt{2}} (1_{2\times 2} - \frac{1}{2} B_2^T B_2 - B_1^T B_2) R_\nu^{(2)} & \frac{1}{\sqrt{2}} (1_{2\times 2} - \frac{1}{2} B_1^T B_1) R_\nu^{(3)} \\ \frac{B_1^T - B_2^T}{\sqrt{2}} R_\nu^{(1)} & -\frac{1}{\sqrt{2}} (1_{2\times 2} - \frac{1}{2} B_2^T B_2 + B_1^T B_2) R_\nu^{(2)} & \frac{1}{\sqrt{2}} (1_{2\times 2} - \frac{1}{2} B_1^T B_1) R_\nu^{(3)} \end{pmatrix} \quad (A22)
\end{aligned}$$

Then, we obtain the relation:

$$\begin{aligned}
R_\nu &= S_\nu R_{1\nu} R_{2\nu} V_\nu \\
&\simeq \begin{pmatrix} R_\nu^{(1)} & -B_2 R_\nu^{(2)} & -B_1 R_\nu^{(3)} \\ \frac{B_1^T + B_2^T}{\sqrt{2}} R_\nu^{(1)} & \frac{1}{\sqrt{2}} (1_{2\times 2} - \frac{1}{2} B_2^T B_2 - B_1^T B_2) R_\nu^{(2)} & \frac{1}{\sqrt{2}} (1_{2\times 2} - \frac{1}{2} B_1^T B_1) R_\nu^{(3)} \\ \frac{B_1^T - B_2^T}{\sqrt{2}} R_\nu^{(1)} & -\frac{1}{\sqrt{2}} (1_{2\times 2} - \frac{1}{2} B_2^T B_2 + B_1^T B_2) R_\nu^{(2)} & \frac{1}{\sqrt{2}} (1_{2\times 2} - \frac{1}{2} B_1^T B_1) R_\nu^{(3)} \end{pmatrix}. \quad (A23)
\end{aligned}$$

On the other hand, using Eq. (A23) we find that the neutrino fields $\nu_L = (\nu_{1L}, \nu_{2L}, \nu_{3L})^T$, $\nu_R^C = (\nu_{1R}^C, \nu_{2R}^C)$ and $N_R^C = (N_{1R}^C, N_{2R}^C)$ are related with the physical neutrino fields by the following relations:

$$\begin{aligned}
\begin{pmatrix} \nu_L \\ \nu_R^C \\ N_R^C \end{pmatrix} &= R_\nu \Psi_L \simeq \begin{pmatrix} R_\nu^{(1)} & -B_2 R_\nu^{(2)} & -B_1 R_\nu^{(3)} \\ \frac{B_1^T + B_2^T}{\sqrt{2}} R_\nu^{(1)} & \frac{1}{\sqrt{2}} (1_{2\times 2} - \frac{1}{2} B_2^T B_2 - B_1^T B_2) R_\nu^{(2)} & \frac{1}{\sqrt{2}} (1_{2\times 2} - \frac{1}{2} B_1^T B_1) R_\nu^{(3)} \\ \frac{B_1^T - B_2^T}{\sqrt{2}} R_\nu^{(1)} & -\frac{1}{\sqrt{2}} (1_{2\times 2} - \frac{1}{2} B_2^T B_2 + B_1^T B_2) R_\nu^{(2)} & \frac{1}{\sqrt{2}} (1_{2\times 2} - \frac{1}{2} B_1^T B_1) R_\nu^{(3)} \end{pmatrix} \begin{pmatrix} \Psi_L^{(1)} \\ \Psi_L^{(2)} \\ \Psi_L^{(3)} \end{pmatrix}, \\
\Psi_L &= \begin{pmatrix} \Psi_L^{(1)} \\ \Psi_L^{(2)} \\ \Psi_L^{(3)} \end{pmatrix}, \quad (A24)
\end{aligned}$$

where $\Psi_{jL}^{(1)}$, $\Psi_{kL}^{(2)} = N_k^+$ and $\Psi_{kL}^{(3)} = N_k^-$ ($j = 1, 2, 3$ and $k = 1, 2$) are the three active neutrinos and four exotic neutrinos, respectively.

[1] Y. Cai, J. Herrero-García, M. A. Schmidt, A. Vicente, and R. R. Volkas, ‘‘From the trees to the forest: a review of radiative neutrino mass models,’’ *Front. in Phys.* **5** (2017) 63, [arXiv:1706.08524](https://arxiv.org/abs/1706.08524) [hep-ph].

- [2] C. Arbeláez, R. Cepedello, J. C. Helo, M. Hirsch, and S. Kovalenko, “How many 1-loop neutrino mass models are there?,” *JHEP* **08** (2022) 023, [arXiv:2205.13063 \[hep-ph\]](#).
- [3] P. Minkowski, “ $\mu \rightarrow e\gamma$ at a Rate of One Out of 10^9 Muon Decays?,” *Phys. Lett. B* **67** (1977) 421–428.
- [4] T. Yanagida, “Horizontal gauge symmetry and masses of neutrinos,” *Conf. Proc. C* **7902131** (1979) 95–99.
- [5] S. L. Glashow, “The Future of Elementary Particle Physics,” *NATO Sci. Ser. B* **61** (1980) 687.
- [6] R. N. Mohapatra and G. Senjanovic, “Neutrino Mass and Spontaneous Parity Nonconservation,” *Phys. Rev. Lett.* **44** (1980) 912.
- [7] M. Gell-Mann, P. Ramond, and R. Slansky, “Complex Spinors and Unified Theories,” *Conf. Proc. C* **790927** (1979) 315–321, [arXiv:1306.4669 \[hep-th\]](#).
- [8] J. Schechter and J. W. F. Valle, “Neutrino Masses in $SU(2) \times U(1)$ Theories,” *Phys. Rev. D* **22** (1980) 2227.
- [9] J. Schechter and J. W. F. Valle, “Neutrino Decay and Spontaneous Violation of Lepton Number,” *Phys. Rev. D* **25** (1982) 774.
- [10] R. N. Mohapatra and J. W. F. Valle, “Neutrino Mass and Baryon Number Nonconservation in Superstring Models,” *Phys. Rev. D* **34** (1986) 1642.
- [11] E. K. Akhmedov, M. Lindner, E. Schnapka, and J. W. F. Valle, “Left-right symmetry breaking in NJL approach,” *Phys. Lett. B* **368** (1996) 270–280, [arXiv:hep-ph/9507275](#).
- [12] E. K. Akhmedov, M. Lindner, E. Schnapka, and J. W. F. Valle, “Dynamical left-right symmetry breaking,” *Phys. Rev. D* **53** (1996) 2752–2780, [arXiv:hep-ph/9509255](#).
- [13] M. Malinsky, J. C. Romao, and J. W. F. Valle, “Novel supersymmetric $SO(10)$ seesaw mechanism,” *Phys. Rev. Lett.* **95** (2005) 161801, [arXiv:hep-ph/0506296](#).
- [14] M. Hirsch, S. Morisi, and J. W. F. Valle, “A4-based tri-bimaximal mixing within inverse and linear seesaw schemes,” *Phys. Lett. B* **679** (2009) 454–459, [arXiv:0905.3056 \[hep-ph\]](#).
- [15] C. O. Dib, G. R. Moreno, and N. A. Neill, “Neutrinos with a linear seesaw mechanism in a scenario of gauged B-L symmetry,” *Phys. Rev. D* **90** no. 11, (2014) 113003, [arXiv:1409.1868 \[hep-ph\]](#).
- [16] M. Chakraborty, H. Z. Devi, and A. Ghosal, “Scaling ansatz with texture zeros in linear seesaw,” *Phys. Lett. B* **741** (2015) 210–216, [arXiv:1410.3276 \[hep-ph\]](#).
- [17] R. Sinha, R. Samanta, and A. Ghosal, “Maximal Zero Textures in Linear and Inverse Seesaw,” *Phys. Lett. B* **759** (2016) 206–213, [arXiv:1508.05227 \[hep-ph\]](#).
- [18] W. Wang and Z.-L. Han, “Radiative linear seesaw model, dark matter, and $U(1)_{B-L}$,” *Phys. Rev. D* **92** (2015) 095001, [arXiv:1508.00706 \[hep-ph\]](#).
- [19] A. E. Cárcamo Hernández, S. Kovalenko, H. N. Long, and I. Schmidt, “A variant of 3-3-1 model for the generation of the SM fermion mass and mixing pattern,” *JHEP* **07** (2018) 144, [arXiv:1705.09169 \[hep-ph\]](#).
- [20] A. E. Cárcamo Hernández, N. A. Pérez-Julve, and Y. Hidalgo Velásquez, “Fermion masses and mixings and some phenomenological aspects of a 3-3-1 model with linear seesaw mechanism,” *Phys. Rev. D* **100** no. 9, (2019) 095025, [arXiv:1907.13083 \[hep-ph\]](#).
- [21] A. E. Cárcamo Hernández, S. Kovalenko, F. S. Queiroz, and Y. S. Villamizar, “An extended 3-3-1 model with radiative linear seesaw mechanism,” *Phys. Lett. B* **829** (2022) 137082, [arXiv:2105.01731 \[hep-ph\]](#).
- [22] A. Batra, P. Bharadwaj, S. Mandal, R. Srivastava, and J. W. F. Valle, “Heavy neutrino signatures from leptophilic Higgs portal in the linear seesaw,” [arXiv:2304.06080 \[hep-ph\]](#).
- [23] A. Batra, P. Bharadwaj, S. Mandal, R. Srivastava, and J. W. F. Valle, “Phenomenology of the simplest linear seesaw mechanism,” [arXiv:2305.00994 \[hep-ph\]](#).
- [24] A. Batra, H. B. Câmara, and F. R. Joaquim, “Dark linear seesaw mechanism,” *Phys. Lett. B* **843** (2023) 138012, [arXiv:2305.01687 \[hep-ph\]](#).
- [25] A. E. Cárcamo Hernández, V. K. N., and J. W. F. Valle, “Linear seesaw mechanism from dark sector,” *JHEP* **09** (2023) 046, [arXiv:2305.02273 \[hep-ph\]](#).
- [26] G. BHATTACHARYYA and D. DAS, “Scalar sector of two-higgs-doublet models: A minireview,” *Pramana* **87** no. 3, (Aug., 2016) . <http://dx.doi.org/10.1007/s12043-016-1252-4>.
- [27] J. Herrero-Garcia, M. Nebot, N. Rius, and A. Santamaria, “The Zee–Babu model revisited in the light of new data,” *Nucl. Phys. B* **885** (2014) 542–570, [arXiv:1402.4491 \[hep-ph\]](#).
- [28] K. L. McDonald and B. H. J. McKellar, “Evaluating the two loop diagram responsible for neutrino mass in Babu’s model,” [arXiv:hep-ph/0309270](#).
- [29] K. Hagiwara, R. Liao, A. D. Martin, D. Nomura, and T. Teubner, “ $(g-2)_\mu$ and $\alpha(M_Z^2)$ re-evaluated using new precise

- data,” *J. Phys.* **G38** (2011) 085003, [arXiv:1105.3149 \[hep-ph\]](#).
- [30] M. Davier, A. Hoecker, B. Malaescu, and Z. Zhang, “Reevaluation of the hadronic vacuum polarisation contributions to the Standard Model predictions of the muon $g - 2$ and $\alpha(m_Z^2)$ using newest hadronic cross-section data,” *Eur. Phys. J. C* **77** no. 12, (2017) 827, [arXiv:1706.09436 \[hep-ph\]](#).
- [31] **RBC, UKQCD** Collaboration, T. Blum, P. A. Boyle, V. Gülpers, T. Izubuchi, L. Jin, C. Jung, A. Jüttner, C. Lehner, A. Portelli, and J. T. Tsang, “Calculation of the hadronic vacuum polarization contribution to the muon anomalous magnetic moment,” *Phys. Rev. Lett.* **121** no. 2, (2018) 022003, [arXiv:1801.07224 \[hep-lat\]](#).
- [32] A. Keshavarzi, D. Nomura, and T. Teubner, “Muon $g - 2$ and $\alpha(M_Z^2)$: a new data-based analysis,” *Phys. Rev.* **D97** no. 11, (2018) 114025, [arXiv:1802.02995 \[hep-ph\]](#).
- [33] T. Aoyama *et al.*, “The anomalous magnetic moment of the muon in the Standard Model,” *Phys. Rept.* **887** (2020) 1–166, [arXiv:2006.04822 \[hep-ph\]](#).
- [34] **Muon g-2** Collaboration, D. P. Aguillard *et al.*, “Measurement of the Positive Muon Anomalous Magnetic Moment to 0.20 ppm,” *Phys. Rev. Lett.* **131** no. 16, (2023) 161802, [arXiv:2308.06230 \[hep-ex\]](#).
- [35] A. E. C. Hernández, D. T. Huong, and I. Schmidt, “Universal inverse seesaw mechanism as a source of the SM fermion mass hierarchy,” *Eur. Phys. J. C* **82** no. 1, (2022) 63, [arXiv:2109.12118 \[hep-ph\]](#).
- [36] L. T. Hue, A. E. Cárcamo Hernández, H. N. Long, and T. T. Hong, “Heavy singly charged Higgs bosons and inverse seesaw neutrinos as origins of large $(g-2)e,\mu$ in two Higgs doublet models,” *Nucl. Phys. B* **984** (2022) 115962, [arXiv:2110.01356 \[hep-ph\]](#).
- [37] A. L. Cherchiglia, G. De Conto, and C. C. Nishi, “Connecting $(g-2)_\mu$ to neutrino mass in the extended neutrinophilic 2HDM,” *JHEP* **08** (2023) 170, [arXiv:2304.00038 \[hep-ph\]](#).
- [38] R. A. Diaz, R. Martinez, and J. A. Rodriguez, “Phenomenology of lepton flavor violation in 2HDM(3) from $(g-2)(\mu)$ and leptonic decays,” *Phys. Rev.* **D67** (2003) 075011, [arXiv:hep-ph/0208117 \[hep-ph\]](#).
- [39] F. Jegerlehner and A. Nyffeler, “The Muon $g-2$,” *Phys. Rept.* **477** (2009) 1–110, [arXiv:0902.3360 \[hep-ph\]](#).
- [40] C. Kelso, H. N. Long, R. Martinez, and F. S. Queiroz, “Connection of $g - 2_\mu$, electroweak, dark matter, and collider constraints on 331 models,” *Phys. Rev.* **D90** no. 11, (2014) 113011, [arXiv:1408.6203 \[hep-ph\]](#).
- [41] M. Lindner, M. Platscher, and F. S. Queiroz, “A Call for New Physics : The Muon Anomalous Magnetic Moment and Lepton Flavor Violation,” *Phys. Rept.* **731** (2018) 1–82, [arXiv:1610.06587 \[hep-ph\]](#).
- [42] K. Kowalska and E. M. Sessolo, “Expectations for the muon $g-2$ in simplified models with dark matter,” *JHEP* **09** (2017) 112, [arXiv:1707.00753 \[hep-ph\]](#).
- [43] G. Bélanger, F. Boudjema, A. Goudelis, A. Pukhov, and B. Zaldivar, “micrOMEGAs5.0 : Freeze-in,” *Computer Physics Communications* **231** (Oct, 2018) 173–186. <https://doi.org/10.1016%2Fj.cpc.2018.04.027>.
- [44] and N. Aghanim, Y. Akrami, M. Ashdown, J. Aumont, C. Baccigalupi, M. Ballardini, A. J. Banday, R. B. Barreiro, N. Bartolo, S. Basak, R. Battye, K. Benabed, J.-P. Bernard, M. Bersanelli, P. Bielewicz, J. J. Bock, J. R. Bond, J. Borrill, F. R. Bouchet, F. Boulanger, M. Bucher, C. Burigana, R. C. Butler, E. Calabrese, J.-F. Cardoso, J. Carron, A. Challinor, H. C. Chiang, J. Chluba, L. P. L. Colombo, C. Combet, D. Contreras, B. P. Crill, F. Cuttaia, P. de Bernardis, G. de Zotti, J. Delabrouille, J.-M. Delouis, E. D. Valentino, J. M. Diego, O. Doré, M. Douspis, A. Ducout, X. Dupac, S. Dusini, G. Efstathiou, F. Elsner, T. A. Enblin, H. K. Eriksen, Y. Fantaye, M. Farhang, J. Fergusson, R. Fernandez-Cobos, F. Finelli, F. Forastieri, M. Frailis, A. A. Fraisse, E. Franceschi, A. Frolov, S. Galeotta, S. Galli, K. Ganga, R. T. Génova-Santos, M. Gerbino, T. Ghosh, J. González-Nuevo, K. M. Górski, S. Gratton, A. Gruppuso, J. E. Gudmundsson, J. Hamann, W. Handley, F. K. Hansen, D. Herranz, S. R. Hildebrandt, E. Hivon, Z. Huang, A. H. Jaffe, W. C. Jones, A. Karakci, E. Keihänen, R. Keskkitalo, K. Kiiveri, J. Kim, T. S. Kisner, L. Knox, N. Krachmalnicoff, M. Kunz, H. Kurki-Suonio, G. Lagache, J.-M. Lamarre, A. Lasenby, M. Lattanzi, C. R. Lawrence, M. L. Jeune, P. Lemos, J. Lesgourgues, F. Levrier, A. Lewis, M. Liguori, P. B. Lilje, M. Lilley, V. Lindholm, M. López-Cañiego, P. M. Lubin, Y.-Z. Ma, J. F. Macías-Pérez, G. Maggio, D. Maino, N. Mandolesi, A. Mangilli, A. Marcos-Caballero, M. Maris, P. G. Martin, M. Martinelli, E. Martínez-González, S. Matarrese, N. Mauri, J. D. McEwen, P. R. Meinhold, A. Melchiorri, A. Mennella, M. Migliaccio, M. Millea, S. Mitra, M.-A. Miville-Deschênes, D. Molinari, L. Montier, G. Morgante, A. Moss, P. Natoli, H. U. Nørgaard-Nielsen, L. Pagano, D. Paoletti, B. Partridge, G. Patanchon, H. V. Peiris, F. Perrotta, V. Pettorino, F. Piacentini, L. Polastri, G. Polenta, J.-L. Puget, J. P. Rachen, M. Reinecke, M. Remazeilles, A. Renzi, G. Rocha, C. Rosset, G. Roudier, J. A. Rubiño-Martín, B. Ruiz-Granados, L. Salvati, M. Sandri, M. Savelainen, D. Scott, E. P. S. Shellard, C. Sirignano, G. Sirri, L. D. Spencer, R. Sunyaev, A.-S. Suur-Uski, J. A. Tauber, D. Tavagnacco, M. Tenti, L. Toffolatti, M. Tomasi, T. Trombetti, L. Valenziano, J. Valiviita, B. V. Tent, L. Vibert, P. Vielva, F. Villa, N. Vittorio, B. D. Wandelt, I. K. Wehus, M. White, S. D. M. White,

- A. Zacchei, and A. Zonca, “Planck 2018 results,”. <https://doi.org/10.1051%2F0004-6361%2F201833910>.
- [45] P. Langacker and D. London, “Lepton Number Violation and Massless Nonorthogonal Neutrinos,” *Phys. Rev. D* **38** (1988) 907.
- [46] L. Lavoura, “General formulae for $f(1) \rightarrow f(2) \gamma$,” *Eur. Phys. J. C* **29** (2003) 191–195, [arXiv:hep-ph/0302221](https://arxiv.org/abs/hep-ph/0302221).
- [47] L. T. Hue, L. D. Ninh, T. T. Thuc, and N. T. T. Dat, “Exact one-loop results for $l_i \rightarrow l_j \gamma$ in 3-3-1 models,” *Eur. Phys. J. C* **78** no. 2, (2018) 128, [arXiv:1708.09723](https://arxiv.org/abs/1708.09723) [hep-ph].
- [48] A. E. C. Hernández and I. Schmidt, “A renormalizable left-right symmetric model with low scale seesaw mechanisms,” *Nucl. Phys. B* **976** (2022) 115696, [arXiv:2101.02718](https://arxiv.org/abs/2101.02718) [hep-ph].
- [49] U. Patel, P. Adarsh, S. Patra, and P. Sahu, “Leptogenesis in a Left-Right Symmetric Model with double seesaw,” *JHEP* **03** (2024) 029, [arXiv:2310.09337](https://arxiv.org/abs/2310.09337) [hep-ph].
- [50] P.-H. Gu and U. Sarkar, “Leptogenesis with Linear, Inverse or Double Seesaw,” *Phys. Lett.* **B694** (2011) 226–232, [arXiv:1007.2323](https://arxiv.org/abs/1007.2323) [hep-ph].
- [51] A. Pilaftsis, “CP violation and baryogenesis due to heavy Majorana neutrinos,” *Phys. Rev.* **D56** (1997) 5431–5451, [arXiv:hep-ph/9707235](https://arxiv.org/abs/hep-ph/9707235) [hep-ph].
- [52] M. J. Dolan, T. P. Dutka, and R. R. Volkas, “Dirac-Phase Thermal Leptogenesis in the extended Type-I Seesaw Model,” *JCAP* **06** (2018) 012, [arXiv:1802.08373](https://arxiv.org/abs/1802.08373) [hep-ph].
- [53] S. Blanchet, T. Hambye, and F.-X. Josse-Michaux, “Reconciling leptogenesis with observable $\mu \rightarrow e \gamma$ rates,” *JHEP* **04** (2010) 023, [arXiv:0912.3153](https://arxiv.org/abs/0912.3153) [hep-ph].
- [54] **Planck** Collaboration, N. Aghanim *et al.*, “Planck 2018 results. VI. Cosmological parameters,” *Astron. Astrophys.* **641** (2020) A6, [arXiv:1807.06209](https://arxiv.org/abs/1807.06209) [astro-ph.CO]. [Erratum: *Astron. Astrophys.* 652, C4 (2021)].